

See discussions, stats, and author profiles for this publication at: <https://www.researchgate.net/publication/234049119>

# Using Binary Surfactant Mixtures To Simultaneously Improve the Dimensional Tunability and Monodispersity in the Seeded Growth of Gold Nanorods

ARTICLE *in* NANO LETTERS · JANUARY 2013

Impact Factor: 13.59 · DOI: 10.1021/nl304478h · Source: PubMed

---

CITATIONS

122

READS

317

## 5 AUTHORS, INCLUDING:



Xingchen Ye

University of California, Berkeley

57 PUBLICATIONS 2,767 CITATIONS

[SEE PROFILE](#)



Chen Zheng

University of Pennsylvania

4 PUBLICATIONS 385 CITATIONS

[SEE PROFILE](#)



Christopher B Murray

University of Pennsylvania

259 PUBLICATIONS 27,581 CITATIONS

[SEE PROFILE](#)

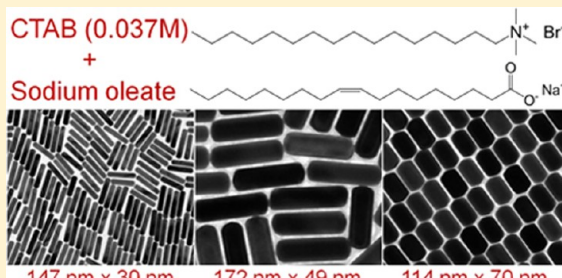
# Using Binary Surfactant Mixtures To Simultaneously Improve the Dimensional Tunability and Monodispersity in the Seeded Growth of Gold Nanorods

Xingchen Ye,<sup>†,§</sup> Chen Zheng,<sup>‡,§</sup> Jun Chen,<sup>†</sup> Yuzhi Gao,<sup>‡</sup> and Christopher B. Murray\*,<sup>†,‡</sup>

<sup>†</sup>Department of Chemistry and <sup>‡</sup>Department of Materials Science and Engineering, University of Pennsylvania, Pennsylvania 19104, United States

## Supporting Information

**ABSTRACT:** We report a dramatically improved synthesis of colloidal gold nanorods (NRs) using a binary surfactant mixture composed of hexadecyltrimethylammonium bromide (CTAB) and sodium oleate (NaOL). Both thin (diameter <25 nm) and thicker (diameter >30 nm) gold NRs with exceptional monodispersity and broadly tunable longitudinal surface plasmon resonance can be synthesized using seeded growth at reduced CTAB concentrations (as low as 0.037 M). The CTAB–NaOL binary surfactant mixture overcomes the difficulty of growing uniform thick gold NRs often associated with the single-component CTAB system and greatly expands the dimensions of gold NRs that are accessible through a one-pot seeded growth process. Gold NRs with large overall dimensions and thus high scattering/absorption ratios are ideal for scattering-based applications such as biolabeling as well as the enhancement of optical processes.



**KEYWORDS:** Gold nanorods, CTAB, sodium oleate, surfactant mixture, tetrahedahedral, plasmonics

Gold nanorods (NRs) have received significant attention in recent years because of great promise for a wide array of applications including plasmon-enhanced spectroscopies,<sup>1,2</sup> bioimaging and therapeutics,<sup>3–5</sup> chemical sensing,<sup>6,7</sup> photonic and optoelectronic devices,<sup>8</sup> and so forth. The resonant excitation of the collective oscillations of free electrons confined to the NRs leads to the creation of localized surface plasmon resonances and large electric field enhancements near the NR surface.<sup>9–11</sup> One of the most intriguing properties of gold NRs is that their longitudinal surface plasmon resonance (LSPR), which can be excited by incident light polarized along the axial direction, depends strongly on the NR aspect ratio and, therefore, can be synthetically tailored across a broad spectral range. Furthermore, the scattering and absorption cross sections at a given LSPR wavelength are largely determined by the overall size of gold NRs.<sup>12</sup> Therefore, the diameter of gold NRs can be an important differentiation factor for their applications. For example, extinction is dominated by absorption for thin gold NRs (diameter less than 15 nm), which makes them well-suited for photothermal applications that require high photon-to-heat conversion efficiency.<sup>13</sup> In contrast, scattering becomes dominant for thicker gold NRs (diameter larger than 30 nm), making them favorable for applications such as biolabeling<sup>14</sup> and enhancement of optical signals including metal-enhanced fluorescence<sup>15</sup> and surface-enhanced spectroscopies,<sup>1,2</sup> and so forth.

Since the seminal reports by Wang et al.,<sup>16</sup> Murphy et al.,<sup>17,18</sup> and El-Sayed and Nikoobakht,<sup>19</sup> seeded growth of colloidal gold NRs in the presence of cationic surfactant CTAB has been

continuously optimized by many research groups.<sup>2,20–30</sup> A variety of additives such as acetone,<sup>17</sup> cyclohexane,<sup>17</sup> Na<sub>2</sub>S,<sup>27</sup> hydrochloric acid or nitric acid,<sup>26,31,32</sup> iodide<sup>33–35</sup> and bromide ions,<sup>36–38</sup> copper ions,<sup>39</sup> and small aromatic molecules<sup>40</sup> have been introduced to the growth solution to affect gold NR growth. Importantly, El-Sayed and Nikoobakht demonstrated that NRs grown in a binary surfactant mixture of CTAB and benzylidimethylhexadecylammoniumchloride (BDAC) can achieve high aspect ratios ranging from 4.6 to 10 after aging of the growth solutions for 7–10 days, which the authors attributed to a more flexible nature of the binary surfactant templates compared to the single-component CTAB system as well as different affinities of the two surfactants on the facets of growing gold NRs.<sup>19</sup> Although nowadays the original idea of using a high concentration of CTAB (0.1 M, far beyond its first critical micelle concentration) as a soft template is not considered the primary role of CTAB during gold NR formation, these previous works suggest that it is possible to achieve greater tunability of NR's dimensions through judicious introduction of additional components to the NR growth solution. On the other hand, significant progress has been made on the size and shape tuning of gold NRs through multistep processes such as direct overgrowth,<sup>2,41,42</sup> transverse overgrowth,<sup>12,43</sup> and anisotropic oxidation<sup>12,44</sup> of preformed gold

**Received:** December 4, 2012

**Revised:** January 1, 2013

**Published:** January 3, 2013



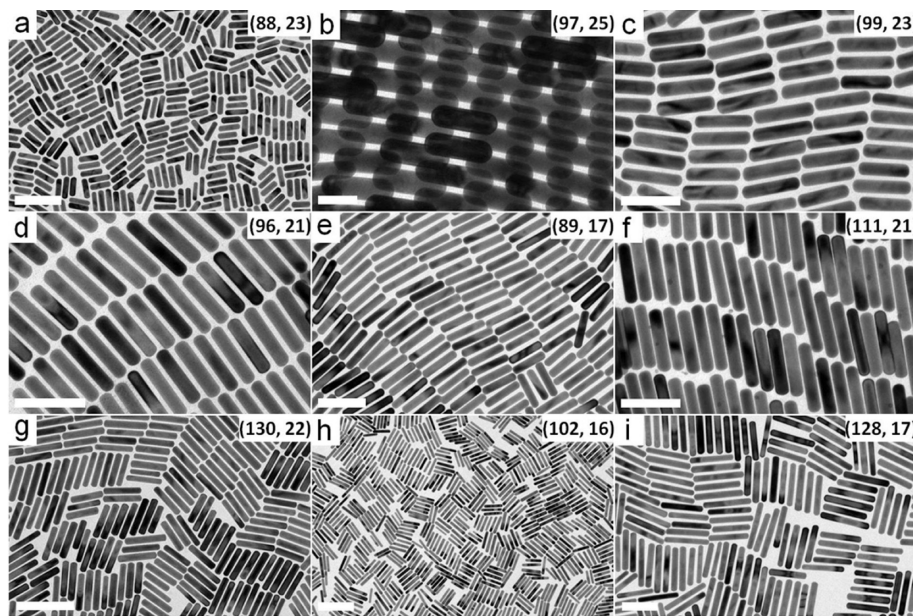


**Figure 1.** (a–i) TEM images of gold NRs having LSPR wavelengths longer than 700 nm and diameters less than 25 nm, arranged in the order of increasing aspect ratio from a to i. Insets are the average length and diameter (in nanometers) of the NRs determined by measuring the dimensions of at least 50 NRs from their TEM images. All NRs were synthesized using 0.037 M CTAB and 0.0078 M NaOL in the growth solution (assuming a total volume of 520 mL), and the growth conditions are detailed in Table S2. Scale bars: (a) 200 nm, (b) 50 nm, (c–f) 100 nm, (g–h) 200 nm, (i) 100 nm.

NRs. Despite these great progress, one-pot seeded growth of monodisperse thick gold NRs (diameter larger than 30 nm) with broadly tunable LSPR has remained quite challenging using existing synthetic procedures.

In this work, we report a dramatic improvement in the seeded growth of colloidal gold nanorods using binary surfactant mixtures. Monodisperse Au NRs with negligible shape impurities (less than 0.5% of the total number of nanoparticles) can be obtained at much lower concentrations of CTAB (as low as 0.037 M) in the NR growth solution compared to the standard protocols (0.1 M). More importantly, the use of a secondary surfactant in addition to CTAB circumvents the limitations in NR's dimensional tunability (particularly NR's diameter) associated with prevailing synthetic procedures, allowing gold NRs having diameters between 15 and 50 nm and LSPR wavelengths tunable from 650 to 1150 nm to be readily accessible in one-pot reactions.

A binary surfactant mixture composed of CTAB and sodium oleate (NaOL) is used in the gold NR growth solution. NaOL, the sodium salt of a long-chain unsaturated fatty acid, is an anionic surfactant soluble in water. The double bond in NaOL molecules allows them to slowly reduce HAuCl<sub>4</sub> in the absence of ascorbic acid (AA), as evidenced by the disappearance of orange–yellow color of dissolved gold salts (detailed synthetic procedures are described in Supporting Information). As a result, the optimal molar ratio between Au(III) and AA is found to be around 3:1 for the CTAB–NaOL system. In contrast, with commonly used methods, HAuCl<sub>4</sub>–CTAB complexes are not reduced until AA is added to the growth solution, and therefore a molar ratio around 1.5 between AA and Au(III) is often employed.

Figure 1 and Figure S2 show TEM images of a collection of monodisperse gold NRs synthesized using 0.037 M CTAB and 0.0126 M NaOL in the growth solution. The aspect ratio of NRs can be continuously adjusted from 3.8 to 7.6 by varying

the amounts of AgNO<sub>3</sub> and seed solutions as well as pH of growth solutions, as detailed in Table S2. Although concentrations of reagents and reaction parameters affect NR dimensions in a complex and interrelated manner, the general trends are: (1) Lowering pH of growth solutions usually leads to a higher NR aspect ratio. A simultaneous increase in NR length and decrease in NR diameter can occur with more acidic growth solutions. Moreover, a greater percent change is often observed in NR diameter at intermediate pH values and in NR length with very acidic growth solutions (pH around 1.0). The trend can be seen by comparing the dimensions of two sets of gold NRs shown in Figure 1 and Figure S2: (1c, 1h, S2d, and 1i) and (1b, 1f, S2c, and 1g), both of which are NR samples synthesized with an increasing acidity of the growth solutions while other experimental conditions were kept unchanged. (2) Reducing the amount of seed particles often results in an increase in both length and diameter of gold NRs (Table S2). Figure 2 shows extinction spectra of the NRs shown in Figure 1. The LSPR wavelength red-shifts from 790 to 1150 nm as the aspect ratio of gold NRs increases. It is notable that a sharp ensemble LSPR is present in every NR sample (e.g., blue curve: fwhm = 110 nm or 0.185 eV for a LSPR at 857 nm; orange curve: fwhm = 130 nm or 0.173 eV for a LSPR at 967 nm; red curve: fwhm = 170 nm or 0.186 eV for a LSPR at 1068 nm), which further confirms the narrow size distribution of NRs. In addition, negligible amounts of shape impurities (e.g., spheres) are produced during NR formation as evidenced by the very weak absorption around 525 nm in the extinction spectra (Figure 2). Gold NRs with a comparable size uniformity and shape purity especially those having LSPR wavelengths longer than 850 nm have rarely been demonstrated with either commonly used methods<sup>19,31,45</sup> or with the CTAB–aromatic additive systems.<sup>40</sup> We further study the growth of gold NRs using 0.047 M CTAB together with NaOL in the growth solution. As shown in Figures S4–S6, a rich array of uniform gold NRs with accessible dimensions comparable to those

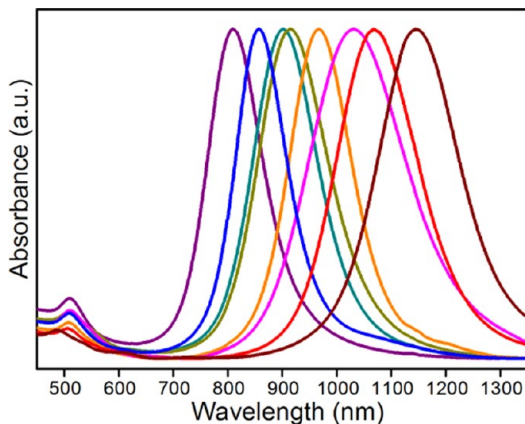


**Figure 2.** Normalized extinction spectra of gold NRs shown in Figure 1. As the NR aspect ratio increases from Figure 1a to i, corresponding LSPR shifts toward longer wavelengths. Spectrum of the sample shown in Figure 1b is not included because it almost overlaps with that of the sample shown in Figure 1a (purple curve).

shown in Figure 1 and Figure S2 can be obtained. It is worth pointing out that gold NRs synthesized using 0.047 M CTAB are consistently smaller in size (especially in diameter) than those made using 0.037 M CTAB provided other reaction conditions are identical (Table S2). This suggests that a high concentration of CTAB may promote NR formation through adsorbing onto the growing gold NRs and selectively blocking

crystal growth along certain directions,<sup>45</sup> which may also be responsible for the limited range of NR dimensions achievable using well-established methods (0.1 M CTAB). Although seed-mediated growth of gold NRs having LSPR wavelength longer than 850 nm has been demonstrated using different strategies such as lowering the pH of growth solutions<sup>31</sup> or using CTAB/BDAC binary surfactants,<sup>19</sup> the diameter of NRs is usually smaller than 20 nm and in most cases, less than 15 nm. On the other hand, as manifested in Figure 1 and Figures S2–S6, the CTAB-NaOL binary mixture may represent an intriguing alternative to the single-component CTAB system since it allows monodisperse high aspect ratio gold NRs having a diameter larger than 20 nm to be generated at comparable pH values of the growth solution.

To explore the possibility of growing thicker gold NRs (diameter >30 nm), we further reduce the amount of seed particles added to the growth solution (Table S3). As shown in Figure 3 and Figure S7, monodisperse gold NRs having diameter between 30 and 45 nm and aspect ratios tunable from 2.2 to 5.0 can be achieved, corresponding to a spectral tunability of NR's LSPR wavelength from 660 to 970 nm (Figure 4). Within the pH range between 1.1 and 1.5 (Table S1), the aspect ratio of gold NRs is largely determined by the acidity of growth solutions (Table S3). NRs of higher aspect ratios are generally attainable using more acidic growth media. The dimensions of gold NRs can be further adjusted by changing the amounts of AgNO<sub>3</sub> or seed particles. Furthermore, a lower concentration of CTAB tends to produce

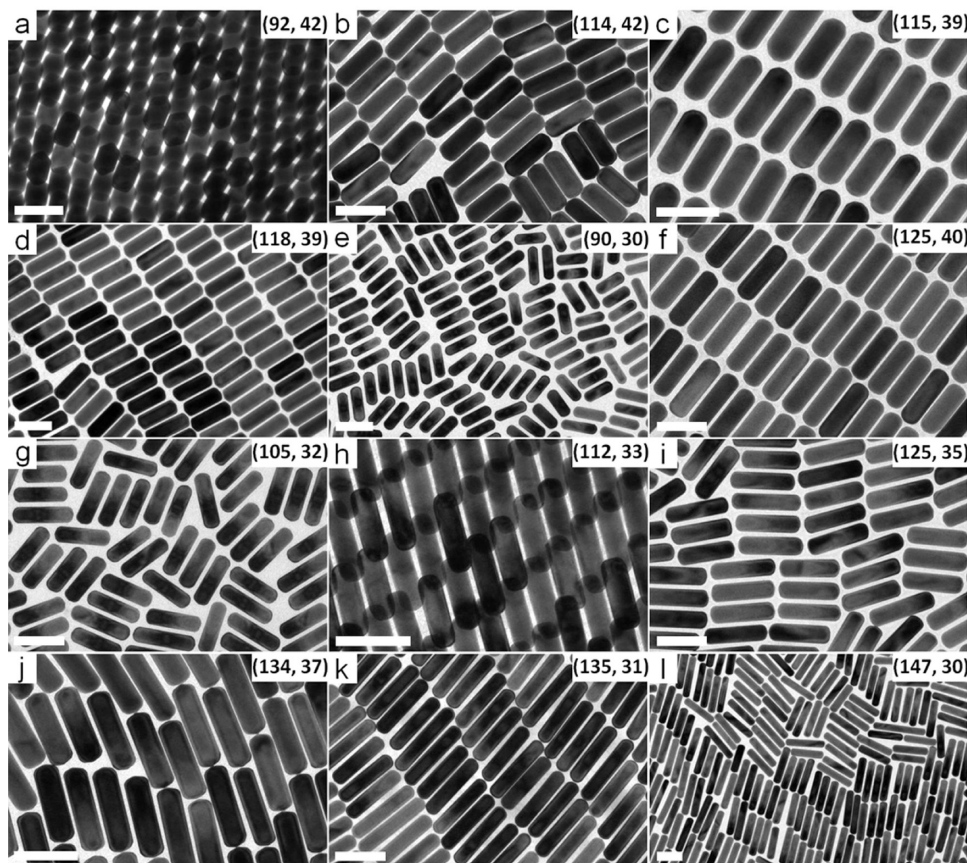


**Figure 3.** (a–l) TEM images of gold NRs having LSPR wavelengths longer than 650 nm and diameters between 25 and 45 nm, arranged in the order of increasing aspect ratio from Figure 1a to l. Insets are the average length and diameter (in nanometers) of the NRs determined by measuring the dimensions of at least 50 NRs from their TEM images. The growth conditions are detailed in Table S3. All scale bars represent 100 nm.

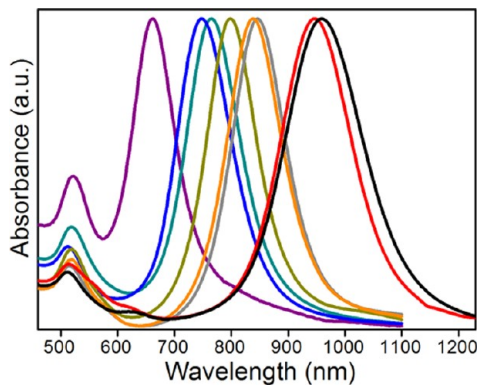


**Figure 4.** Normalized extinction spectra of gold NRs shown in Figure 3a (purple curve), 3c (blue curve), 3d (dark cyan curve), 3f (dark yellow curve), 3i (orange curve), 3j (gray curve), 3k (red curve), and 3l (black curve).

thicker NRs. For example, NRs shown in Figure 3c (made with 0.037 M CTAB) are larger in diameter than those in Figure 3h.

(made with 0.047 M CTAB), even though the latter are made with fewer seed particles present in the growth solution.

Using the CTAB–NaOL binary surfactant mixture, even thicker gold NRs (diameter >45 nm) can be obtained as the seed volume is further reduced (Figures 5, 6, S8–S10, and Tables S4–S5). The combination of a minimum amount of seed particles and a fairly acidic growth solution ( $\text{pH} = 1.10$ ) yields gold NRs with an aspect ratio as high as 3.4 (Figure 5f), resulting in an LSPR centered at 895 nm (Figure 5h, blue curve). Figure 7 displays the extinction spectra of those thick gold NRs of similar aspect ratios as shown in Figure 6a–d. When the diameter of gold NRs is greater than a critical value, which is found to be about 50 nm, a further increase in NR's diameter leads to a gradual red-shift of the transverse plasmon band and a concomitant decrease in the ratio of intensities between the longitudinal and transverse plasmonic resonances (Figure 7). As dimensions of gold NRs become larger, they start to develop clear faceting. Morphological studies using SEM show that thick gold NRs (diameter <100 nm) are elongated tetrahedrahedral (ETHH) shaped, which is consistent

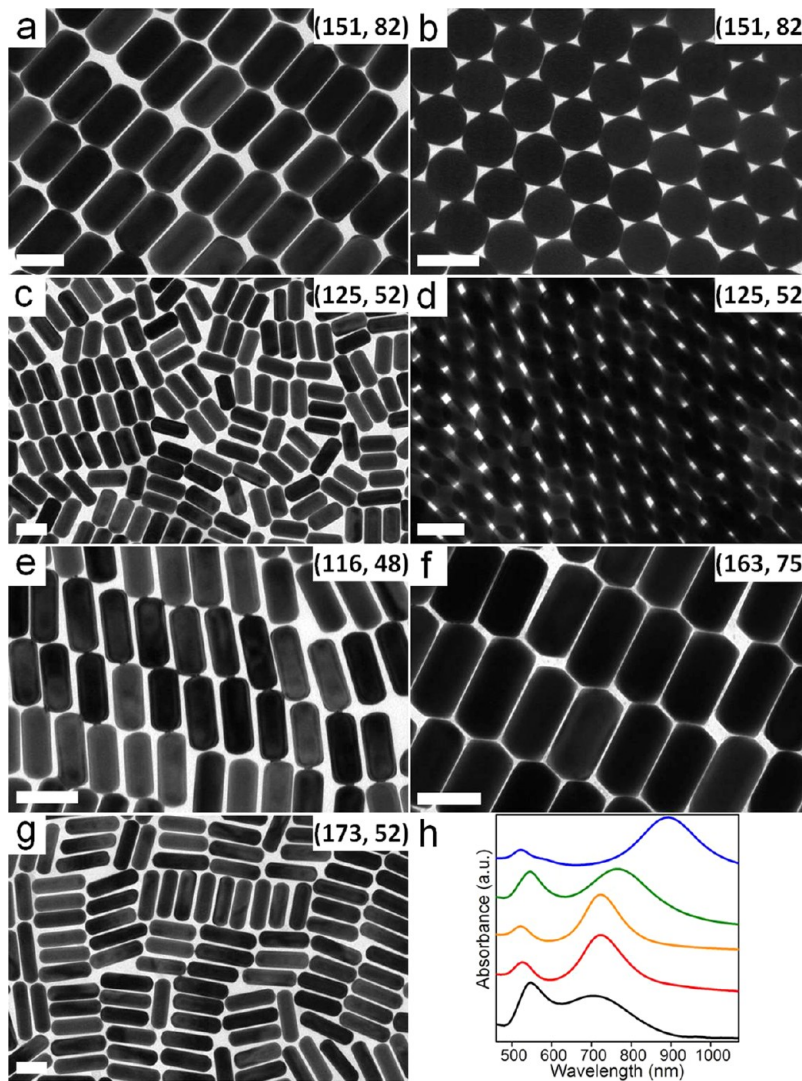


**Figure 5.** (a–g) TEM images of gold NRs having LSPR wavelengths longer than 700 nm and diameters greater than 45 nm. Insets are the average length and diameter (in nanometers) of the NRs determined by measuring the dimensions of at least 50 NRs from their TEM images. The growth conditions are detailed in Table S4. (h) Normalized extinction spectra of gold NRs shown in a–b (black curve), c–d (red curve), e (orange curve), f (green curve), and g (blue curve), respectively. All scale bars represent 100 nm. The spectra have been offset vertically for clarity.

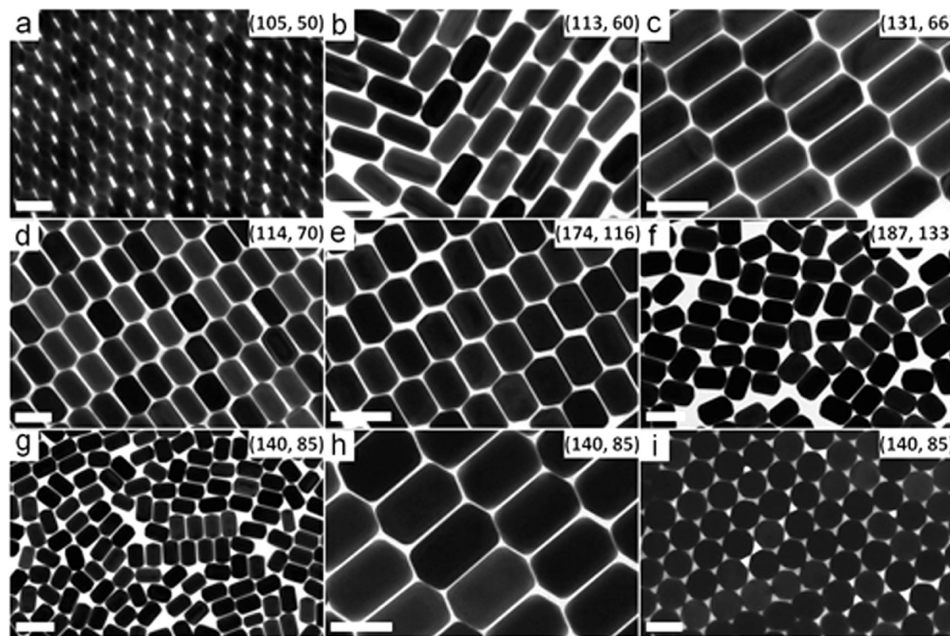


**Figure 6.** (a–i) TEM images of gold NRs having LSPR wavelengths shorter than 700 nm and diameters greater than 50 nm. Insets are the average length and diameter (in nm) of the NRs determined by measuring the dimensions of at least 50 NRs from their TEM images. The growth conditions are detailed in Table S5. Scale bars: (a–d) 100 nm, (e–g) 200 nm, (h–i) 100 nm.

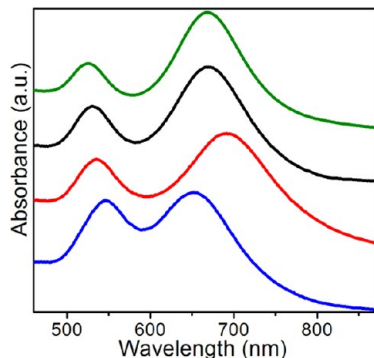


**Figure 7.** Normalized extinction spectra of gold NRs shown in Figure 6a (green curve), 6b (black curve), 6c (red curve), and 6d (blue curve). The spectra have been offset vertically for clarity.

with previous reports of ETHH gold nanocrystals (Figure 8a–c and Figure S11).<sup>46–48</sup> However, we do observe that, in thicker gold NRs (diameter >100 nm), additional truncations or facetings occur at the eight vertices where six facets meet on the ETHH NRs, giving rise to a total of 32 exposed facets as opposed to 24 as for an ETHH nanocrystal (Figure 8d–f).

To shed more light on gold NR formation in the CTAB–NaOL binary surfactant mixtures, a series of control experiments are conducted. First, the cationic species of the oleate surfactant does not seem to influence the growth of gold NRs, as shown by the fact that NRs of similar dimensions and comparable quality can be synthesized by replacing NaOL with the same amount of potassium oleate as long as all other experimental parameters are kept identical (Figure S13). Second, replacing NaOL with other long-chain unsaturated surfactants such as sodium linoleate (having two double bonds) or oleylamine also leads to reduction of Au(III) to Au(I) before the addition of AA. In both cases, gold NRs can still be produced at high yields, albeit with slightly inferior size uniformity and shape purity (Figure S14). The reducing power

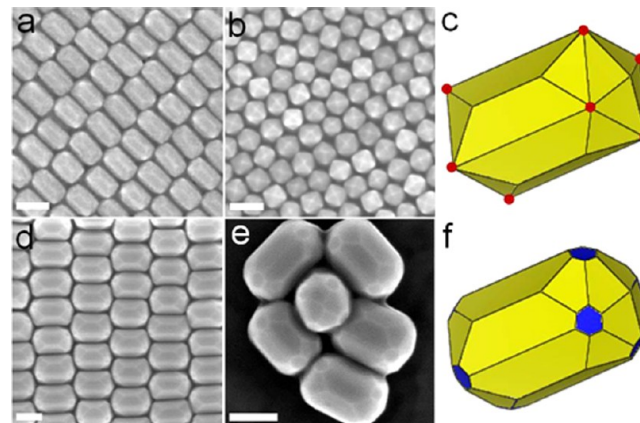


**Figure 8.** SEM images of (a) horizontally and (b) vertically aligned gold NRs (the same sample shown in Figure 6d) having dimensions of  $(114.2 \pm 5.1)$  nm  $\times$   $(69.8 \pm 3.1)$  nm and (c) structural model of ETHH NRs. Red dots: vertices where six facets meet. (d–e) SEM images of gold NRs (the same sample shown in Figure 6e) having dimensions of  $(173.7 \pm 9.1)$  nm  $\times$   $(115.6 \pm 4.0)$  nm and (f) structural model of truncated ETHH NRs. All scale bars represent 100 nm.

of double bond in NaOL molecules toward Au(III) at room temperature is further confirmed by the absence of color disappearance when using sodium stearate, the saturated structural analogue of NaOL. With sodium stearate, even though the same amount of AA as common methods (4.5 mL of 0.064 M AA solution at our scale) is added, the yield of gold NRs is still very low, and the amount of spheroidal impurities is significant (Figure S15). Third, uniform gold NRs can only be produced with an acidic growth media using the CTAB–NaOL system ( $\text{pH} < 1.7$ ). Since NaOL is a basic salt, adjusting the pH through addition of HCl is essential for gold NR formation (Figure S16a–c). Fourthly, same level of control over NR's size uniformity as well as tunability in NR's dimensions is hardly achievable using the standard method (0.1 M CTAB) given

comparable acidities ( $\text{pH} < 1.5$ ) of NR growth solutions (Figure S17). At a similar pH, the yield of gold NRs drops dramatically when 0.047 M CTAB is used in the absence of NaOL (Figure S16d). Moreover, no gold NR formation occurs after 48 h when the amount of AA is further reduced to  $[\text{Au(III)}]:[\text{AA}] = 4:1$ . Therefore, in the CTAB–NaOL binary surfactant system, a small amount of AA is still necessary to reduce  $\text{Au(I)}$  to  $\text{Au}^0$  catalyzed by the seed particles. Furthermore, reducing  $\text{Au(III)}$  to  $\text{Au(I)}$  is not the sole role of NaOL. As shown in Table S6, a slight increase in the amount of NaOL (1 mmol) in the growth solution (without a measurable pH increase) consistently results in an increase in the diameter of gold NRs, provided all other growth conditions are kept the same. This suggests that NaOL molecules might mediate the binding between CTAB surfactants and certain facets of growing NRs.

In summary, we demonstrated that by using a binary surfactant mixture composed of CTAB and NaOL, gold NRs with simultaneously improved dimensional tunability and size uniformity compared to conventional methods can be synthesized while reducing the concentration of CTAB (as low as 0.037 M). Not only thin gold NRs (diameter smaller than 25 nm) with exceptional monodispersity and broadly tunable LSPRs can be made, but more importantly, thick gold NRs (diameter larger than 30 nm) with aspect ratios tunable up to 5.0 can be synthesized using seed-mediated growth. Although the LSPR wavelength of gold NRs is largely determined by their aspect ratios, the dimensions of NRs provide an effective means of tailoring the relative proportions of absorption and scattering that make up the extinction observed for the NRs at the LSPR frequency.<sup>12</sup> The CTAB–NaOL binary surfactant mixture overcomes the difficulty of growing monodisperse thick gold NRs associated with the single-component CTAB system and greatly expands the dimensions of gold NRs that are accessible through a one-pot seeded growth process. Gold NRs with large overall dimensions and thus high scattering/absorption ratios are ideal for studies on plasmonic coupling<sup>1,49</sup> as well as scattering-based applications such as biolabeling<sup>14</sup> as well as enhancement of optical signals.<sup>1,2,15</sup>

## ■ ASSOCIATED CONTENT

### S Supporting Information

Methods and detailed reaction conditions, additional TEM and SEM images, photographs of seed solution and nanorod growth solution, dark-field scattering image, and results of control experiments. This material is available free of charge via the Internet at <http://pubs.acs.org>.

## ■ AUTHOR INFORMATION

### Corresponding Author

\*E-mail: cbmurray@sas.upenn.edu.

### Author Contributions

<sup>§</sup>These authors contributed equally to this work.

### Notes

The authors declare no competing financial interest.

## ■ ACKNOWLEDGMENTS

X.Y., C.Z., Y.G., and C.B.M. acknowledge the support from the Office of Naval Research (ONR) Multidisciplinary University Research Initiative (MURI) on Optical Metamaterials through award N00014-10-1-0942. J.C. acknowledges the support from

the MRSEC program of the National Science Foundation under award no. DMR 11-20901. C.B.M. is also grateful to the Richard Perry University Professorship for support of his supervisor role. We thank Jamie Ford and Douglas Yates at the Penn Regional Nanotechnology Facility for support in SEM.

## ■ REFERENCES

- (1) Halas, N. J.; Lal, S.; Chang, W.-S.; Link, S.; Nordlander, P. *Chem. Rev.* **2011**, *111*, 3913–3961.
- (2) Alvarez-Puebla, R. A.; Agarwal, A.; Manna, P.; Khanal, B. P.; Aldeanueva-Potel, P.; Carbo-Argibay, E.; Pazos-Perez, N.; Vigdeman, L.; Zubarev, E. R.; Kotov, N. A.; Liz-Marzan, L. *Proc. Natl. Acad. Sci. U.S.A.* **2011**, *108*, 8157–8161.
- (3) Wijaya, A.; Schaffer, S. B.; Pallares, I. G.; Hamad-Schifferli, K. *ACS Nano* **2009**, *3*, 80–86.
- (4) Dreaden, E. C.; Alkilany, A. M.; Huang, X.; Murphy, C. J.; El-Sayed, M. A. *Chem. Soc. Rev.* **2012**, *41*, 2740–2779.
- (5) Cobley, C. M.; Chen, J.; Cho, E. C.; Wang, L. V.; Xia, Y. *Chem. Soc. Rev.* **2011**, *40*, 44–56.
- (6) Kabashin, A. V.; Evans, P.; Pastkovsky, S.; Hendren, W.; Wurtz, G. A.; Atkinson, R.; Pollard, R.; Podolskiy, V. A.; Zayats, A. V. *Nat. Mater.* **2009**, *8*, 867–871.
- (7) Liu, N.; Tang, M. L.; Hentschel, M.; Giessen, H.; Alivisatos, A. P. *Nat. Mater.* **2011**, *10*, 631–636.
- (8) Knight, M. W.; Sobhani, H.; Nordlander, P.; Halas, N. J. *Science* **2011**, *332*, 702–704.
- (9) P Perez-Juste, J.; Pastoriza-Santos, I.; Liz-Marzan, L. M.; Mulvaney, P. *Coord. Chem. Rev.* **2005**, *249*, 1870–1901.
- (10) Vigdeman, L.; Khanal, B. P.; Zubarev, E. R. *Adv. Mater.* **2012**, *24*, 4811–4841.
- (11) Chen, H.; Shao, L.; Li, Q.; Wang, J. *Chem. Soc. Rev.* **2013**, DOI: 10.1039/C2CS35367A.
- (12) Ni, W.; Kou, X.; Yang, Z.; Wang, J. F. *ACS Nano* **2008**, *2*, 677–686.
- (13) Huang, X.; Neretina, S.; El-Sayed, M. A. *Adv. Mater.* **2009**, *21*, 4880–4910.
- (14) Rostro-Kohanloo, B. C.; Bickford, L. R.; Payne, C. M.; Day, E. S.; Anderson, L. J. E.; Zhong, M.; Lee, S.; Mayer, K. M.; Zal, T.; Adam, L.; Dinney, C. P. N.; Drezek, R. A.; West, J. L.; Hafner, J. H. *Nanotechnology* **2009**, *20*, 434005.
- (15) Lakowicz, J. R.; Ray, K.; Chowdhury, M.; Szmacinski, H.; Fu, Y.; Zhang, J.; Nowaczky, K. *Analyst* **2008**, *133*, 1308–1346.
- (16) Yu, Y. Y.; Chang, S. S.; Lee, C. L.; Wang, C. R. C. *J. Phys. Chem. B* **1997**, *101*, 6661.
- (17) Jana, N. R.; Gearheart, L.; Murphy, C. J. *Adv. Mater.* **2001**, *13*, 1389–1393.
- (18) Jana, N. R.; Gearheart, L.; Murphy, C. J. *J. Phys. Chem. B* **2001**, *105*, 4065–4067.
- (19) Nikoobakht, B.; El-Sayed, M. A. *Chem. Mater.* **2003**, *15*, 1957–1962.
- (20) Busbee, B. D.; Obare, S. O.; Murphy, C. J. *Adv. Mater.* **2003**, *15*, 414–416.
- (21) Gole, A.; Murphy, C. J. *Chem. Mater.* **2004**, *16*, 3633–3640.
- (22) Sau, T. K.; Murphy, C. J. *Langmuir* **2004**, *20*, 6414–6420.
- (23) Liu, M. Z.; Guyot-Sionnest, P. *J. Phys. Chem. B* **2005**, *109*, 22192–22200.
- (24) Perez-Juste, J.; Liz-Marzan, L. M.; Carnie, S.; Chan, D. Y. C.; Mulvaney, P. *Adv. Funct. Mater.* **2004**, *14*, 571–579.
- (25) Taub, N.; Krichevski, O.; Markovich, G. *J. Phys. Chem. B* **2003**, *107*, 11579–11582.
- (26) Wu, H. Y.; Chu, H. C.; Kuo, T. J.; Kuo, C. L.; Huang, M. H. *Chem. Mater.* **2005**, *17*, 6447–6451.
- (27) Zweifel, D. A.; Wei, A. *Chem. Mater.* **2005**, *17*, 4256–4261.
- (28) Jiang, X. C.; Brioude, A.; Pilani, M. P. *Colloids Surf., A* **2006**, *277*, 201–206.
- (29) Kou, X. S.; Zhang, S. Z.; Tsung, C. K.; Yang, Z.; Yeung, M. H.; Stucky, G. D.; Sun, L. D.; Wang, J. F.; Yan, C. H. *Chem.—Eur. J.* **2007**, *13*, 2929–2936.

- (30) Guerrero-Martinez, A.; Perez-Juste, J.; Carbo-Argibay, E.; Tardajos, G.; Liz-Marzan, L. M. *Angew. Chem., Int. Ed.* **2009**, *48*, 9484–9488.
- (31) Zhu, J.; Yong, K.-T.; Roy, I.; Hu, R.; Ding, H.; Zhao, L.; Swihart, M. T.; He, G. S.; Cui, Y.; Prasad, P. N. *Nanotechnology* **2010**, *21*, 285106.
- (32) Kim, F.; Sohn, K.; Wu, J.; Huang, J. *J. Am. Chem. Soc.* **2008**, *130*, 14442–14443.
- (33) Smith, D. K.; Miller, N. R.; Korgel, B. A. *Langmuir* **2009**, *25*, 9518–9524.
- (34) Smith, D. K.; Korgel, B. A. *Langmuir* **2008**, *24*, 644–649.
- (35) Rayavarapu, R. G.; Ungureanu, C.; Krystek, P.; van Leeuwen, T. G.; Manohar, S. *Langmuir* **2010**, *26*, 5050–5055.
- (36) Sau, T. K.; Murphy, C. J. *Philos. Mag.* **2007**, *87*, 2143–2158.
- (37) Garg, N.; Scholl, C.; Mohanty, A.; Jin, R. C. *Langmuir* **2010**, *26*, 10271–10276.
- (38) Si, S.; Leduc, C.; Delville, M.-H.; Lounis, B. *ChemPhysChem* **2012**, *13*, 193–202.
- (39) Wen, T.; Hu, Z.; Liu, W.; Zhang, H.; Hou, S.; Hu, X.; Wu, X. *Langmuir* **2012**, DOI: 10.1021/la304181k.
- (40) Ye, X.; Jin, L.; Caglayan, H.; Chen, J.; Xing, G.; Zheng, C.; Doan-Nguyen, V.; Kang, Y.; Engheta, N.; Kagan, C. R.; Murray, C. B. *ACS Nano* **2012**, *6*, 2804–2817.
- (41) Song, J. H.; Kim, F.; Kim, D.; Yang, P. *Chem.—Eur. J.* **2005**, *11*, 910–916.
- (42) Sohn, K.; Kim, F.; Pradel, K. C.; Wu, J.; Peng, Y.; Zhou, F.; Huang, J. *ACS Nano* **2009**, *3*, 2191–2198.
- (43) Kou, X. S.; Zhang, S. Z.; Yang, Z.; Tsung, C. K.; Stucky, G. D.; Sun, L. D.; Wang, J. F.; Yan, C. H. *J. Am. Chem. Soc.* **2007**, *129*, 6402–6404.
- (44) Tsung, C. K.; Kou, X. S.; Shi, Q. H.; Zhang, J. P.; Yeung, M. H.; Wang, J. F.; Stucky, G. D. *J. Am. Chem. Soc.* **2006**, *128*, 5352–5353.
- (45) Murphy, C. J.; Thompson, L. B.; Chernak, D. J.; Yang, J. A.; Sivapalan, S. T.; Boulos, S. P.; Huang, J. Y.; Alkilany, A. M.; Sisco, P. N. *Curr. Opin. Colloid Interface Sci.* **2011**, *16*, 128–134.
- (46) Ming, T.; Feng, W.; Tang, Q.; Wang, F.; Sun, L.; Wang, J.; Yan, C. *J. Am. Chem. Soc.* **2009**, *131*, 16350–16351.
- (47) Yin, P.-G.; You, T.-T.; Tan, E.-Z.; Li, J.; Lang, X.-F.; Jiang, L.; Guo, L. *J. Phys. Chem. C* **2011**, *115*, 18061–18069.
- (48) Kim, D. Y.; Im, S. H.; Park, O. O. *Cryst. Growth Des.* **2010**, *10*, 3321–3323.
- (49) Funston, A. M.; Novo, C.; Davis, T. J.; Mulvaney, P. *Nano Lett.* **2009**, *9*, 1651–1658.

*Supporting information for:*

# **Using Binary Surfactant Mixtures to Simultaneously Improve Dimensional Tunability and Monodispersity in the Seeded-Growth of Gold Nanorods**

*Xingchen Ye<sup>1†</sup>, Chen Zheng<sup>2†</sup>, Jun Chen<sup>1</sup>, Yuzhi Gao<sup>2</sup>, Christopher B. Murray<sup>1, 2\*</sup>*

<sup>1</sup>Department of Chemistry and <sup>2</sup>Department of Materials Science and Engineering, University of Pennsylvania, Pennsylvania 19104, United States.

<sup>†</sup>These authors contributed equally to this work

\*To whom correspondence should be addressed. E-mail: [cbmurray@sas.upenn.edu](mailto:cbmurray@sas.upenn.edu)

## Methods

**Materials.** All chemicals were obtained from commercial suppliers and used without further purification. Hexadecyltrimethylammonium bromide (CTAB, > 98.0%), sodium oleate (NaOL, > 97.0%), potassium oleate (KOL, > 98.0%), sodium linoleate (> 95.0%), sodium stearate (> 95.0%) were purchased from TCI America. Hydrogen tetrachloroaurate trihydrate ( $\text{HAuCl}_4 \cdot 3\text{H}_2\text{O}$ ) were purchased from Acros Organics. L-ascorbic Acid (BioUltra,  $\geq 99.5\%$ ), silver nitrate ( $\text{AgNO}_3$ , >99%), sodium borohydride ( $\text{NaBH}_4$ , 99%), oleylamine (technical grade, 70%) and hydrochloric acid (HCl, 37 wt. % in water) were purchased from Sigma Aldrich. Ultrapure water obtained from a Milli-Q Integral 5 system was used in all experiments. All glassware was cleaned using freshly prepared aqua regia (HCl:  $\text{HNO}_3$  in a 3:1 ratio by volume) followed by rinsing with copious amounts of water.

**Synthesis of Gold NRs.** The seed solution for gold NR growth was prepared as follows: 5 mL of 0.5 mM  $\text{HAuCl}_4$  was mixed with 5 mL of 0.2 M CTAB solution in a 20 mL scintillation vial. 0.6 mL of fresh 0.01 M  $\text{NaBH}_4$  was diluted to 1 mL with water and was then injected to the Au(III)-CTAB solution under vigorous stirring (1200 rpm). The solution color changed from yellow to brownish yellow and the stirring was stopped after 2 min. The seed solution was aged at room temperature for 30 min before use.

To prepare the growth solution, 7.0 g (0.037 M in the final growth solution) or 9.0 g (0.047 M in the final growth solution) of CTAB and a certain quantity of NaOL were dissolved in 250 mL of warm water ( $\sim 50^\circ\text{C}$ ) in a 1L Erlenmeyer flask (Tables S2-S5). The solution was allowed to cool down to 30  $^\circ\text{C}$  and 4 mM  $\text{AgNO}_3$  solution, as detailed in Tables S2-S5, was added. The mixture was kept undisturbed at 30  $^\circ\text{C}$  for 15 min after which 250 mL of 1 mM  $\text{HAuCl}_4$  solution

was added. The solution became colorless after 90 min of stirring (700 rpm) and a certain volume of HCl (37 wt. % in water, 12.1 M) was then introduced to adjust the pH (Tables S2-S5). After another 15 min of slow stirring at 400 rpm, 1.25 mL of 0.064 M ascorbic acid (AA) was added and the solution was vigorously stirred for 30 s. Finally, a small amount of seed solution was injected into the growth solution (Tables S2-S5). The resultant mixture was stirred for 30 s and left undisturbed at 30°C for 12 h for NR growth. The final products were isolated by centrifugation at 7,000 rpm for 30 min followed by removal of the supernatant. No size and/or shape-selective fractionation was performed.

**Structural and Optical Characterization.** Transmission electron microscopy (TEM) images were acquired on a JEM-1400 microscope operating at 120kV. Scanning electron microscopy (SEM) was performed on a JEOL 7500F HRSEM operating at 5.0 kV. Optical extinction spectra were recorded using a Cary 5000 UV/Vis/NIR spectrophotometer. The pH of NR growth solutions were measured with an accument AP72 pH meter (Fisher Scientific). Dark-field imaging was carried out on an Olympus BX51 upright optical microscope. Samples were prepared by drop-casting a diluted solution of gold NRs (~20 µL) onto a piece of clean glass cover slip, and were illuminated by white light from a 100 W tungsten-halogen lamp through an oil immersion dark-field condenser (NA 1.2–1.4). The scattered light was collected using a 50x objective (NA 0.75) and the images were captured with a color digital camera on a 308 PV microscope spectrophotometer system (Craic Technologies).



**Figure S1.** Photograph of a typical seed solution. To prepare high quality seed particles, it is crucial that the amount of NaBH<sub>4</sub> added for HAuCl<sub>4</sub> reduction is precise. Since NaBH<sub>4</sub> is very hygroscopic, it is highly recommended that NaBH<sub>4</sub> powders are stored in a N<sub>2</sub>-purged glovebox. Moreover, although we found that ice-cold NaBH<sub>4</sub> (aq) is not necessary, it is important to use fresh NaBH<sub>4</sub> (aq) (used within 2 min after its preparation).

**Table S1.** pH values of gold NR growth solutions with different amounts of added HCl.<sup>a</sup>

volume of HCl (37 wt. % in water, 12.1 M)	pH <sup>b</sup>
N/A	5.86±0.12
1.0 mL	1.65±0.04
1.5 mL	1.51±0.02
2.1 mL	1.36±0.03
3.0 mL	1.27±0.04
3.6 mL	1.10±0.02
4.2 mL	1.06±0.01
4.8 mL	1.03±0.02
5.4 mL	0.95±0.01

<sup>a</sup> The pH values are nearly identical between gold NR growth solutions using 1.234g (4 mmol) and 1.543g (~5 mmol) of NaOL given the same amount of added HCl.

<sup>b</sup> Average values and standard deviations were determined by measuring the pH values of 10 batches of gold NR growth solutions having identical concentrations of reagents.

**Table S2.** Growth conditions for gold NRs with LSPR wavelengths longer than 700 nm and diameters less than 25 nm.

CTAB (g)	AgNO <sub>3</sub> (mL)	Seed (mL)	HCl (mL)	NaOL (g)	Average length (nm)	Average diameter (nm)	Figure number
7.0	18.0	0.4	1.5	1.234	88.1±3.9	23.4±1.0	1a
7.0	18.0	0.8	2.1	1.234	89.3±4.1	16.7±0.8	1e, S3
7.0	18.0	0.4	2.1	1.234	95.9±5.2	21.2±1.5	1d
7.0	18.0	0.8	3.0	1.234	94.2±6.7	16.2±1.2	S2a
7.0	18.0	0.2	3.0	1.234	111.4±8.2	23.3±1.3	S2b
7.0	24.0	0.8	2.1	1.234	98.9±5.2	22.7±0.9	1c
7.0	24.0	0.4	2.1	1.234	97.2±4.9	25.1±1.2	1b
7.0	24.0	0.8	3.0	1.234	93.9±6.2	16.5±1.0	S14f
7.0	24.0	0.4	3.0	1.234	111.4±6.0	20.8±0.8	1f
7.0	24.0	0.8	3.6	1.234	101.5±5.5	15.5±0.7	1h
7.0	24.0	0.4	3.6	1.234	118.4±6.4	19.7±1.1	S2c
7.0	24.0	0.8	4.8	1.234	107.5±7.2	14.7±0.6	S2d
7.0	24.0	0.4	4.8	1.234	129.7±6.1	21.6±1.6	1g
7.0	24.0	0.8	5.4	1.234	127.8±7.0	16.8±0.9	1i
9.0	18.0	0.4	3.0	1.234	86.9±3.6	21.2±1.3	S6
9.0	18.0	0.2	3.0	1.543	109.5±5.7	27.3±1.9	S2e

9.0	24.0	0.4	2.1	1.543	92.2±4.8	22.1±1.1	S2f
9.0	12.0	0.8	2.1	1.234	69.9±3.7	17.5±0.9	S14i
9.0	18.0	0.4	1.5	1.234	86.7±5.1	20.0±1.4	S5
9.0	18.0	0.2	1.5	1.234	94.1±4.3	24.2±1.0	S5
9.0	18.0	0.2	2.1	1.234	98.2±6.2	23.8±1.1	S6
9.0	18.0	0.2	3.0	1.234	118.4±8.3	22.7±1.6	S6
9.0	24.0	0.8	1.5	1.234	86.0±4.2	16.4±0.9	S4
9.0	24.0	0.4	1.5	1.234	91.2±5.8	18.3±1.0	S4, S5
9.0	24.0	0.2	1.5	1.234	106.3±6.7	27.1±1.3	S4, S5
9.0	24.0	0.8	2.1	1.234	89.6±4.5	15.2±0.8	S4
9.0	24.0	0.4	2.1	1.234	104.3±5.0	18.0±0.6	S4
9.0	24.0	0.2	2.1	1.234	119.0±7.0	24.0±1.4	S4, S6
9.0	24.0	0.8	3.0	1.234	86.1±3.7	14.3±0.4	S4
9.0	24.0	0.2	3.0	1.234	126.2±6.9	23.7±1.1	S4, S6
9.0	24.0	0.2	4.2	1.234	137.1±8.3	24.2±1.4	S4
9.0	36.0	0.4	1.5	1.234	94.3±4.1	19.6±0.9	S5, S13b
9.0	36.0	0.2	2.1	1.234	110.0±6.2	22.7±1.0	S6
9.0	36.0	0.4	3.0	1.234	113.7±6.0	16.2±0.7	S6
9.0	36.0	0.2	3.0	1.234	122.0±7.8	19.8±0.7	S6

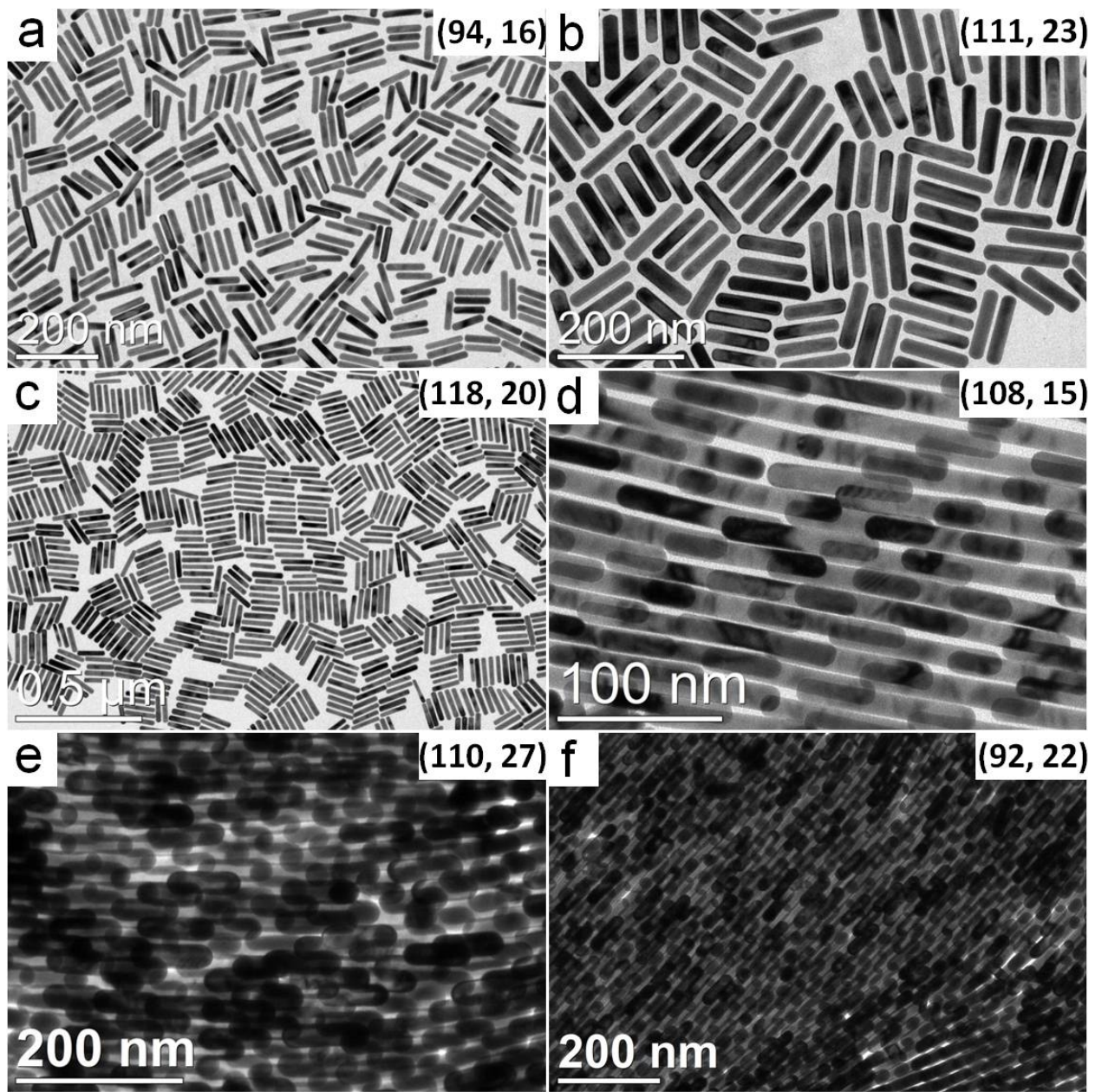


**Figure S2.** (a-f) TEM images of gold NRs having LSPR wavelengths longer than 700 nm and diameters less than 30 nm. Insets are the average length and diameter (in nm) of the NRs determined by measuring the dimensions of at least 50 NRs from their TEM images. NR growth conditions are detailed in Table S2.

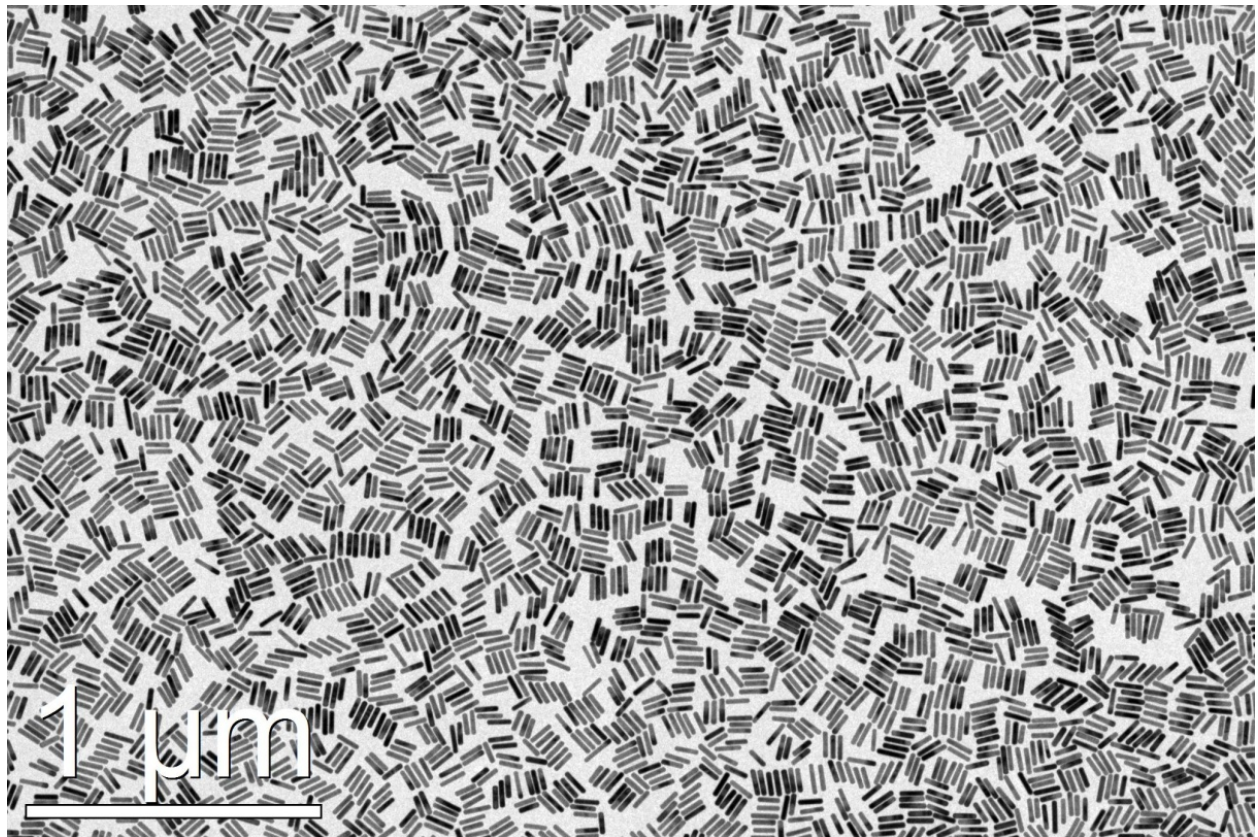


**Figure S3.** Large area TEM image of the same gold NRs shown in Figure 1e. The dimensions of the NRs are  $(89.3 \pm 4.1)$  nm x  $(16.7 \pm 0.8)$  nm. The growth conditions are detailed in Table S2.

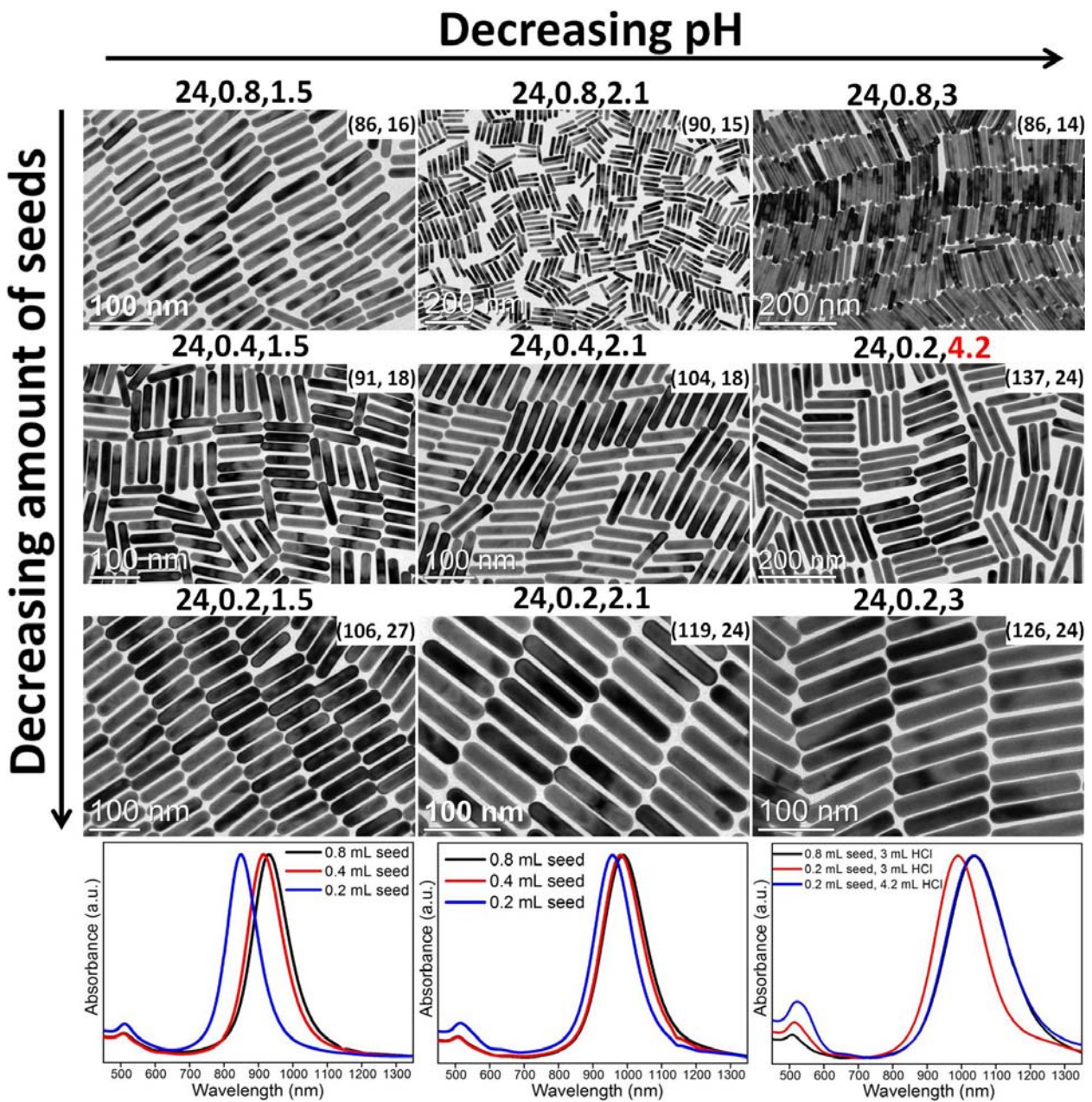


**Figure S4.** TEM images of gold NRs having LSPR wavelengths longer than 700 nm and diameters less than 30 nm. Insets are the average length and diameter (in nm) of the NRs determined by measuring the dimensions of at least 50 NRs from their TEM images. All NRs were synthesized using 0.047 M CTAB and 1.234 g of NaOL in the growth solution. The amounts (in mL) of 4mM AgNO<sub>3</sub> solution, seed solution and HCl added to the growth solution are provided above the TEM image of corresponding NR sample. Normalized extinction spectra of gold NRs are shown at the bottom of each column.

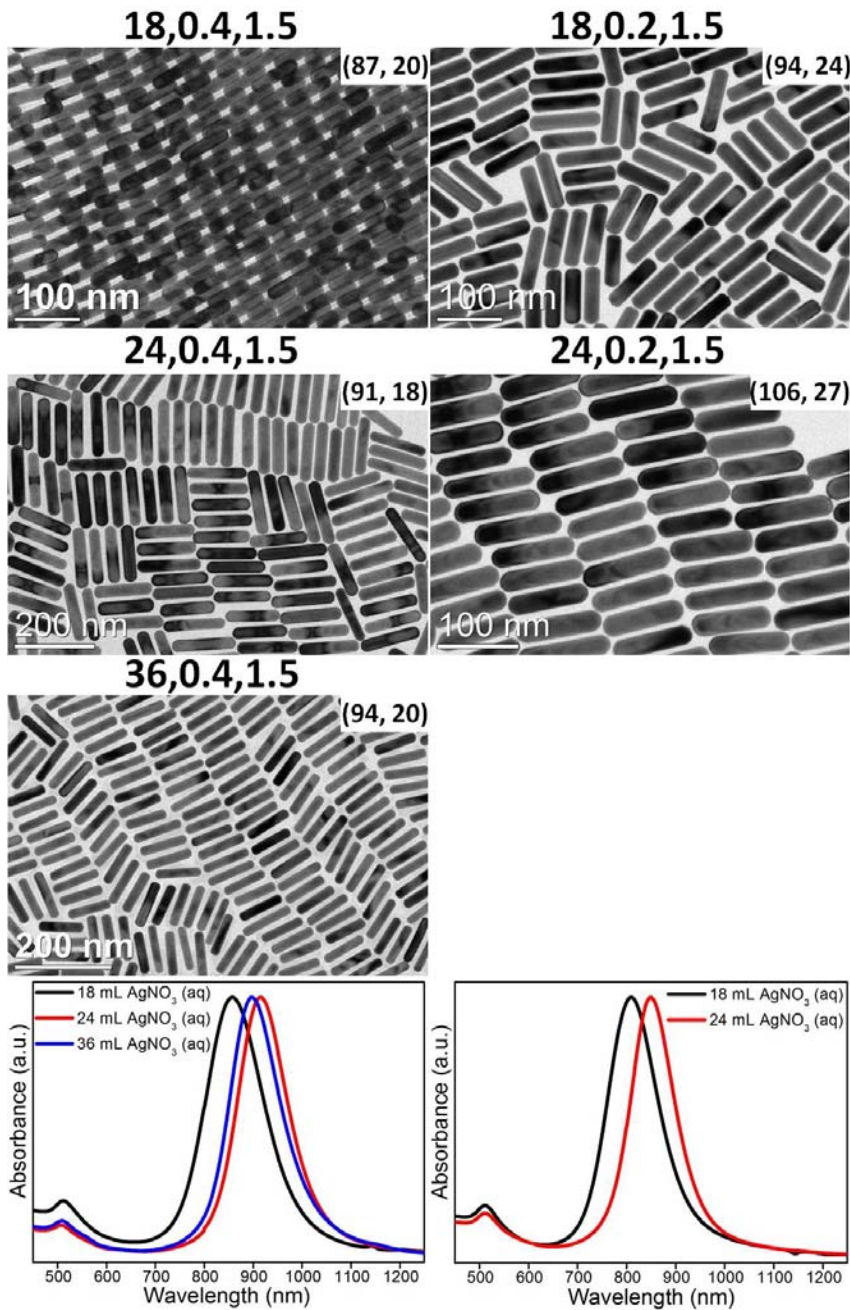


**Figure S5.** TEM images of gold NRs having LSPR wavelengths longer than 700 nm and diameters less than 30 nm. Insets are the average length and diameter (in nm) of the NRs determined by measuring the dimensions of at least 50 NRs from their TEM images. All NRs were synthesized using ~0.047M CTAB and 1.234 g of NaOL in the growth solution. The amounts (in mL) of 4mM AgNO<sub>3</sub> solution, seed solution and HCl added to the growth solution are provided above the TEM image of corresponding NR sample. Normalized extinction spectra of gold NRs are shown at the bottom of each column.

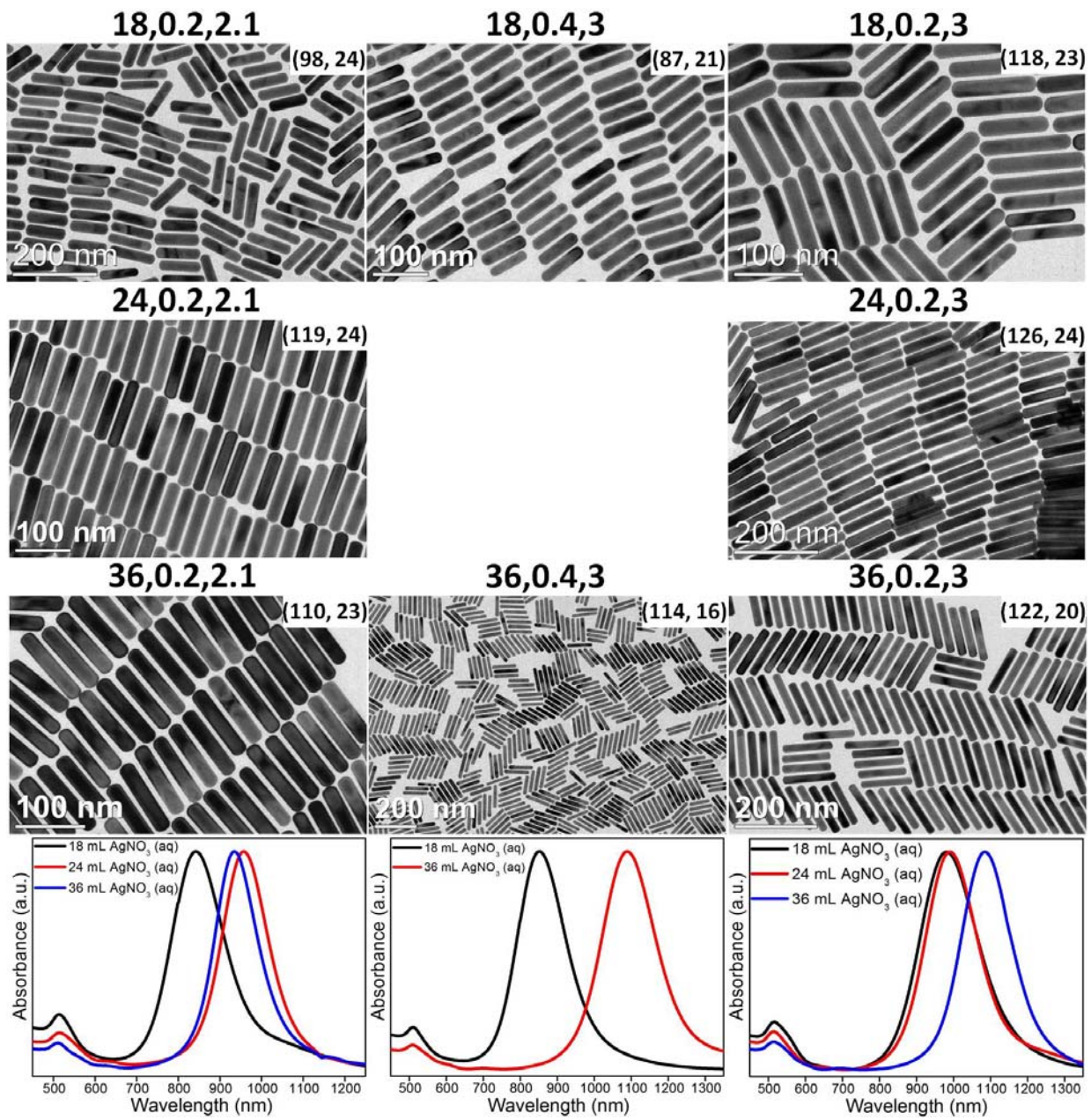


**Figure S6.** TEM images of gold NRs having LSPR wavelengths longer than 700 nm and diameters less than 30 nm. Insets are the average length and diameter (in nm) of the NRs determined by measuring the dimensions of at least 50 NRs from their TEM images. All NRs were synthesized using ~0.047M CTAB and 1.234 g of NaOL in the growth solution. The amounts (in mL) of 4mM AgNO<sub>3</sub> solution, seed solution and HCl added to the growth solution are provided above the TEM image of corresponding NR sample. Normalized extinction spectra of gold NRs are shown at the bottom of each column.

**Table S3.** Growth conditions for gold NRs with LSPR wavelengths longer than 650 nm and diameters between 25 and 45 nm.

CTAB (g)	AgNO <sub>3</sub> (mL)	Seed (mL)	HCl (mL)	NaOL (g)	Average length (nm)	Average diameter (nm)	Figure number
7.0	12.0	0.8	2.1	1.234	91.7±4.3	41.8±2.2	3a
7.0	24.0	0.4	1.5	1.234	115.1±6.4	38.7±1.6	3c
7.0	24.0	0.1	3.0	1.543	122.1±7.5	41.2±3.3	S7a
9.0	18.0	0.05	1.5	1.234	118.8±4.6	38.9±2.4	3d
9.0	18.0	0.4	2.1	1.543	90.0±3.0	30.1±1.1	3e
9.0	18.0	0.2	2.1	1.543	99.1±6.1	35.7±2.0	S7b
9.0	24.0	0.2	1.5	1.234	111.8±5.0	33.2±1.3	3h, S7c
9.0	24.0	0.1	1.5	1.234	125.0±5.5	40.1±1.9	3f
9.0	24.0	0.2	2.1	1.234	119.0±7.0	24.0±1.4	S4
9.0	24.0	0.1	2.1	1.234	124.8±6.6	34.7±1.8	3i
9.0	24.0	0.2	3.0	1.234	129.4±8.2	31.4±2.5	S7d
9.0	24.0	0.05	3.0	1.234	134.9±8.0	30.7±1.8	3k, S7e
9.0	24.0	0.05	3.6	1.234	142.8±6.5	30.1±1.9	S7f
9.0	24.0	0.05	4.2	1.234	147.0±6.3	29.6±1.2	3l

9.0	24.0	0.2	1.5	1.543	$113.7 \pm 6.2$	$41.8 \pm 2.4$	3b, S7g
9.0	24.0	0.2	2.1	1.543	$105.0 \pm 5.7$	$32.2 \pm 1.7$	3g
9.0	24.0	0.2	3.0	1.543	$113.8 \pm 5.4$	$25.2 \pm 1.2$	S7h
9.0	30.0	0.2	1.5	1.234	$106.5 \pm 6.8$	$28.2 \pm 1.8$	S7i
9.0	36.0	0.2	3.0	1.234	$131.5 \pm 5.5$	$27.4 \pm 1.6$	S7j
9.0	48.0	0.2	2.1	1.234	$122.9 \pm 7.8$	$28.7 \pm 2.0$	S7k
9.0	48.0	0.1	2.1	1.234	$134.3 \pm 7.3$	$37.1 \pm 2.2$	3j

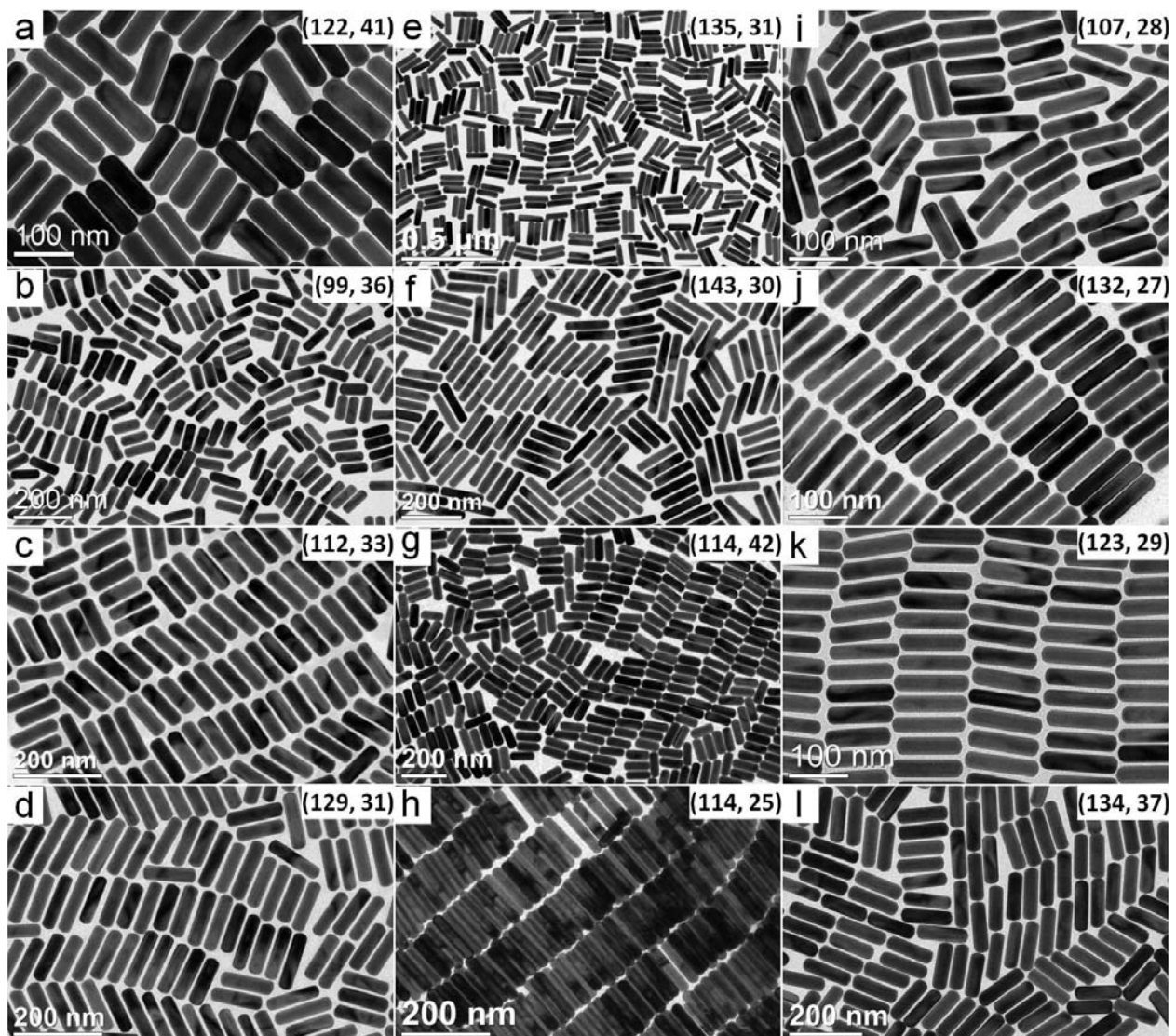


**Figure S7.** (a-l) TEM images of gold NRs having LSPR wavelengths longer than 650 nm and diameters between 30 and 45 nm. Insets are the average length and diameter (in nm) of the NRs determined by measuring the dimensions of at least 50 NRs from their TEM images. NR growth conditions are detailed in Table S3.

**Table S4.** Growth conditions for gold NRs with LSPR wavelengths longer than 700 nm and diameters greater than 45 nm.

CTAB (g)	AgNO <sub>3</sub> (mL)	Seed (mL)	HCl (mL)	NaOL (g)	Average length (nm)	Average diameter (nm)	Figure number
7.0	12.0	0.8	2.1	1.543	109.2±9.1	54.4±3.0	S8a
7.0	24.0	0.2	1.5	1.234	124.7±7.8	52.2±2.1	5c, 5d
9.0	18.0	0.01	1.5	1.234	151.4±8.3	81.7±4.3	5a, 5b, S11c
9.0	24.0	0.01	3.0	1.234	171.9±12.3	48.9±3.0	S8c, S8d
9.0	24.0	0.01	3.6	1.234	173.3±8.0	51.8±2.6	5g, S8b
9.0	24.0	0.1	1.5	1.543	115.7±5.9	47.9±1.9	5e
9.0	24.0	0.01	3.0	1.543	163.0±10.7	74.9±4.0	5f

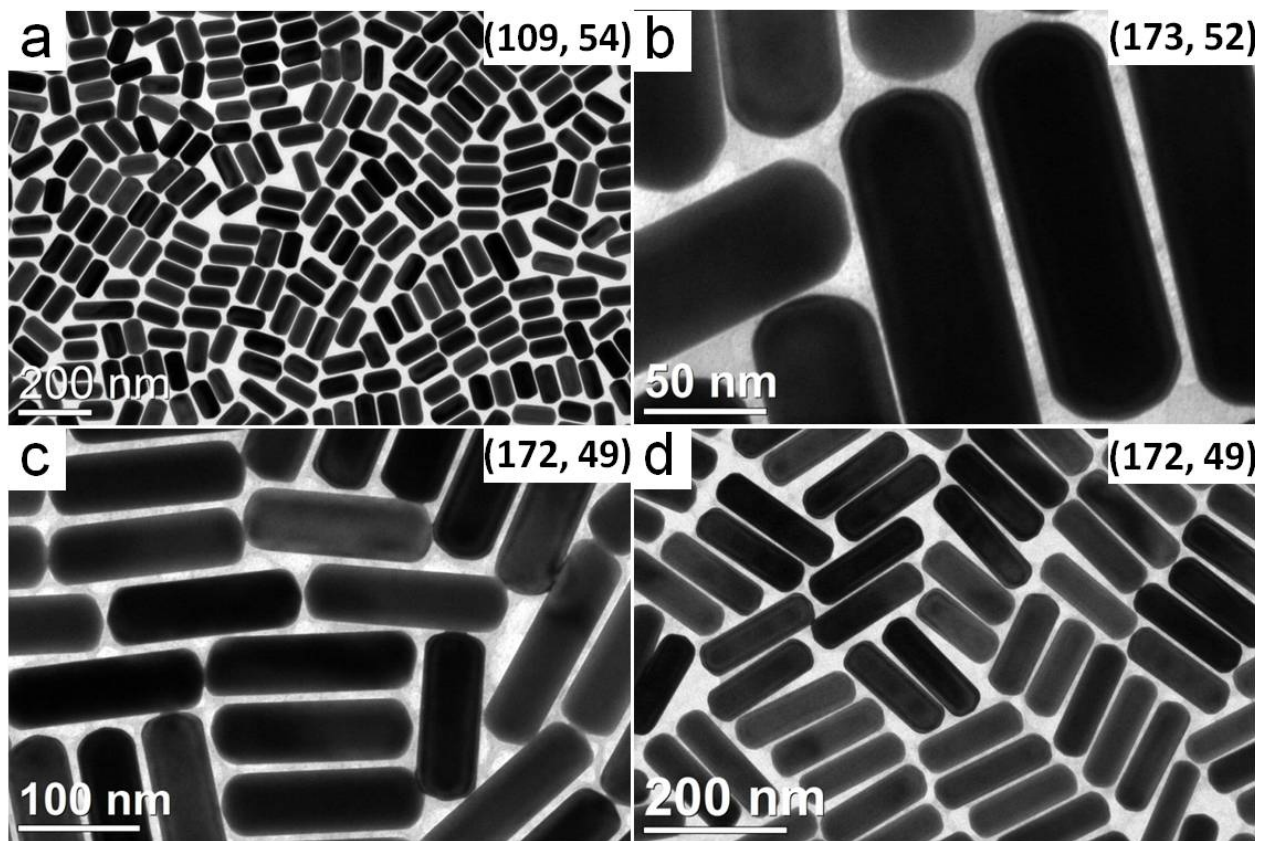


**Figure S8.** (a-d) TEM images of gold NRs having LSPR wavelengths longer than 700 nm and diameters greater than 45 nm. Insets are the average length and diameter (in nm) of the NRs determined by measuring the dimensions of at least 50 NRs from their TEM images. NR growth conditions are detailed in Table S4.

**Table S5.** Growth conditions for gold NRs with LSPR wavelengths shorter than 700 nm and diameters greater than 50 nm.

CTAB (g)	AgNO <sub>3</sub> (mL)	Seed (mL)	HCl (mL)	NaOL (g)	Average length (nm)	Average diameter (nm)	Figure number
7.0	12.0	0.2	1.0	1.234	114.1±6.8	63.2±3.4	S10a, S10b
7.0	12.0	0.2	1.5	1.234	101.7±5.0	58.5±2.8	S10c, S10d
7.0	12.0	0.2	2.1	1.543	187.2±10.5	133.6±6.0	6f
7.0	12.0	0.2	3.0	1.543	115.4±6.2	64.6±3.0	S10e
7.0	18.0	0.4	1.5	1.234	140.0±5.0	84.7±3.7	6g-i, S9, S11a-b, S14c
7.0	18.0	0.2	1.5	1.234	113.0±4.9	59.6±2.6	6b, S11g
9.0	12.0	0.8	1.0	1.543	110.0±8.9	69.8±3.8	S10f
9.0	12.0	0.05	1.5	1.543	114.2±5.1	69.8±3.1	6d, 8a, 8b, S11d-f
9.0	12.0	0.01	1.5	1.543	173.7±9.1	115.6±4.0	6e, 8d, 8e
9.0	12.0	0.01	2.1	1.543	136.0±8.8	80.0±5.5	S10g, S10h
9.0	12.0	0.01	3.0	1.543	131.3±5.8	66.0±3.4	6c
9.0	18.0	0.4	1.5	1.543	88.2±4.0	40.0±1.6	S10i, S10j
9.0	18.0	0.2	1.5	1.543	105.3±4.5	49.9±2.0	6a, S11h, S11i

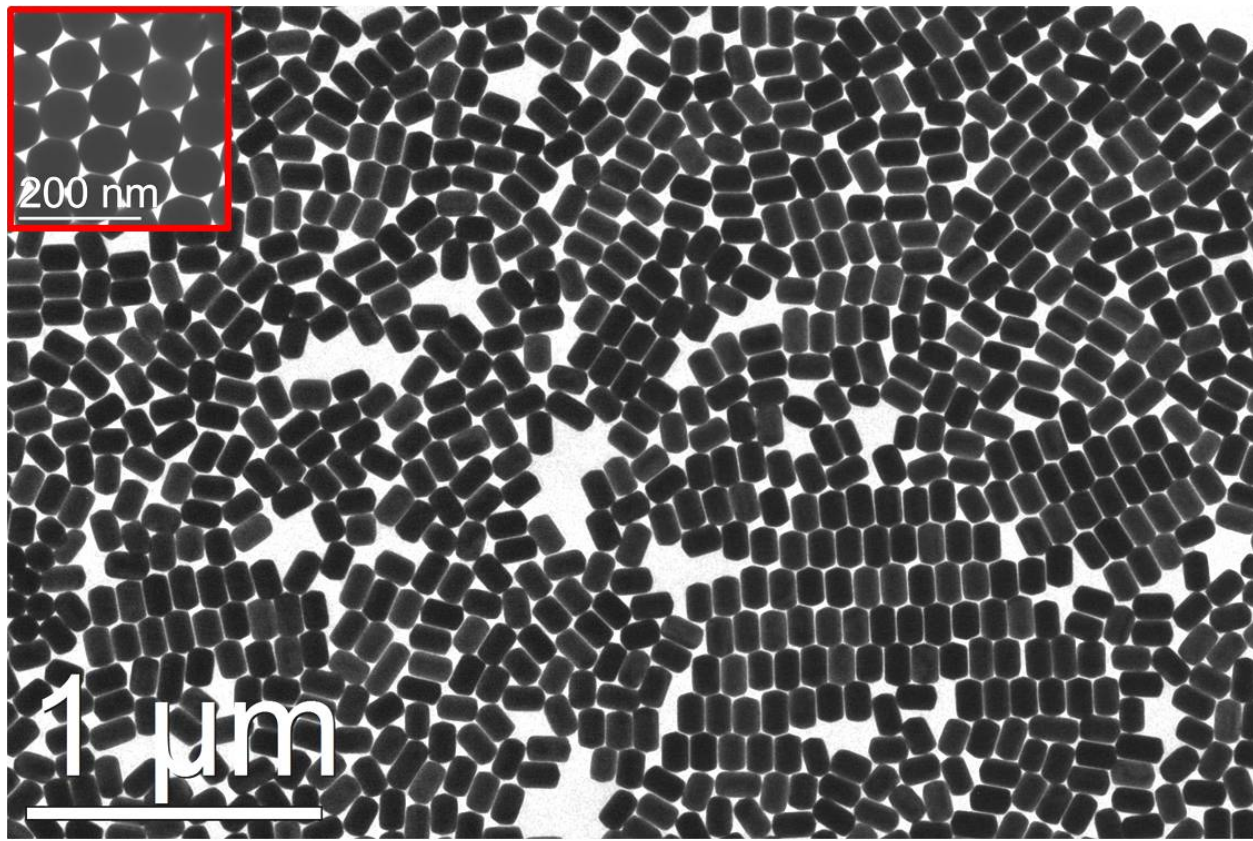


**Figure S9.** Large area TEM image of the same gold NRs shown in Figures 6g-i. The dimensions of the NRs are  $(140.0 \pm 5.0)$  nm x  $(84.7 \pm 3.7)$  nm. The growth conditions are detailed in Table S5.

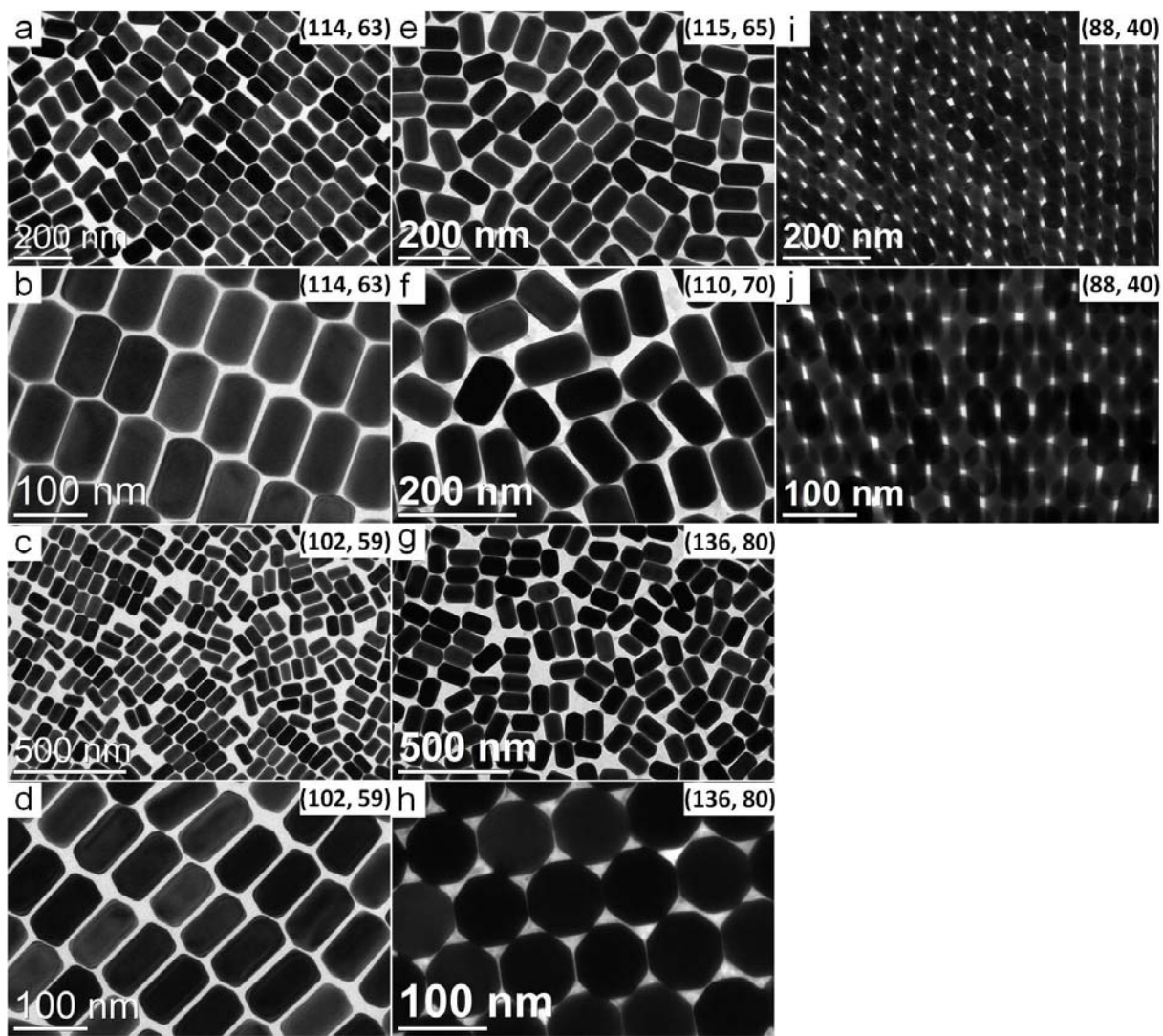


**Figure S10.** (a-j) TEM images of gold NRs having LSPR wavelengths shorter than 700 nm and diameters greater than 40 nm. Insets are the average length and diameter (in nm) of the NRs determined by measuring the dimensions of at least 50 NRs from their TEM images. NR growth conditions are detailed in Table S5.

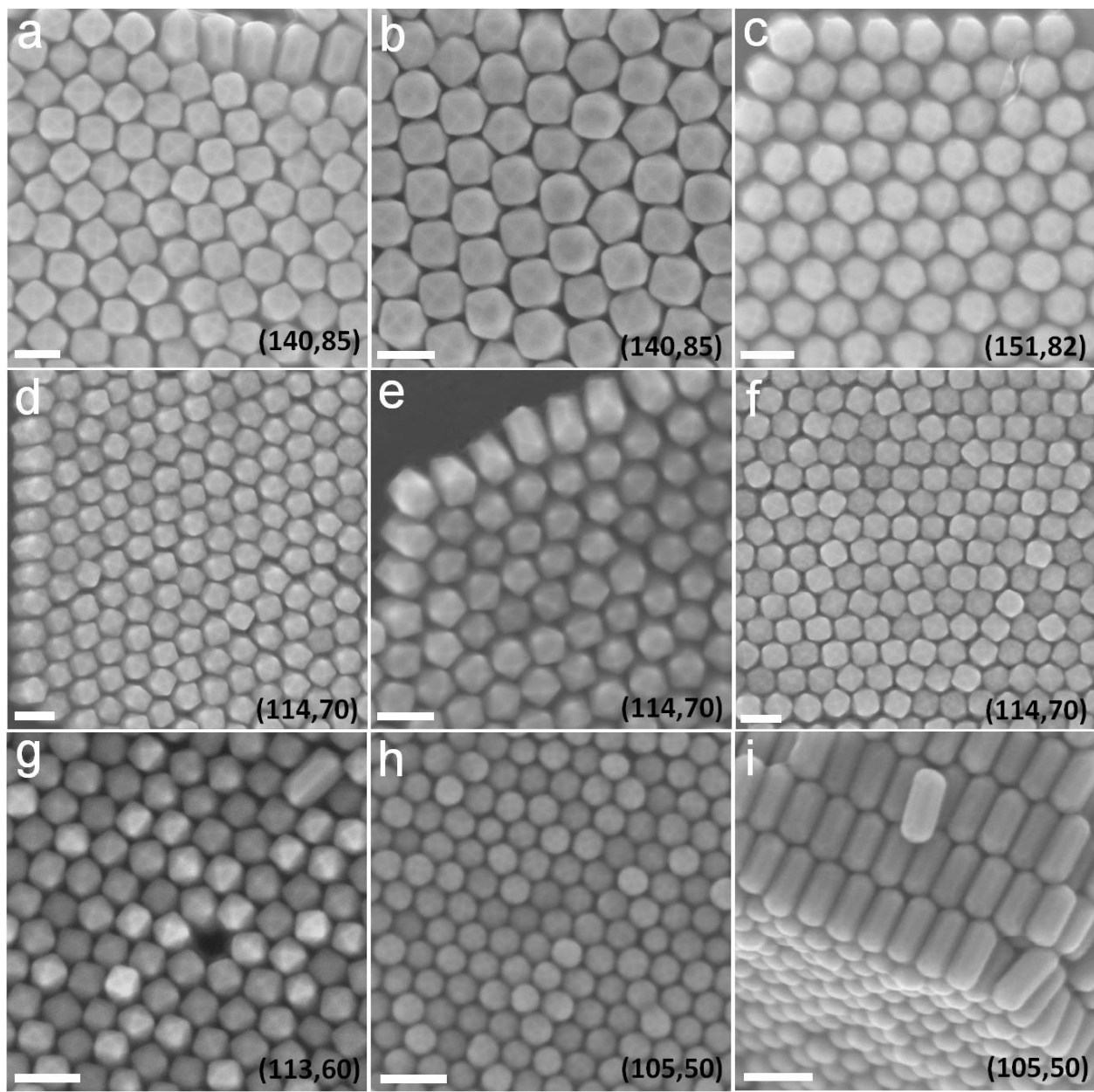


**Figure S11.** Additional SEM images of ETTH-shaped gold NRs having LSPR wavelengths shorter than 700 nm and diameters greater than 50 nm. Insets are the average length and diameter (in nm) of the NRs determined by measuring the dimensions of at least 50 NRs from their TEM images. All scale bars represent 100 nm. Correlations between the same sample's TEM and SEM image are: (a, b) Figures 6g-i and Figure S9. (c) Figures 5a, 5b. (d-f) Figures 6d, 8a, 8b. (g) Figure 6b. (h, i) Figure 6a.

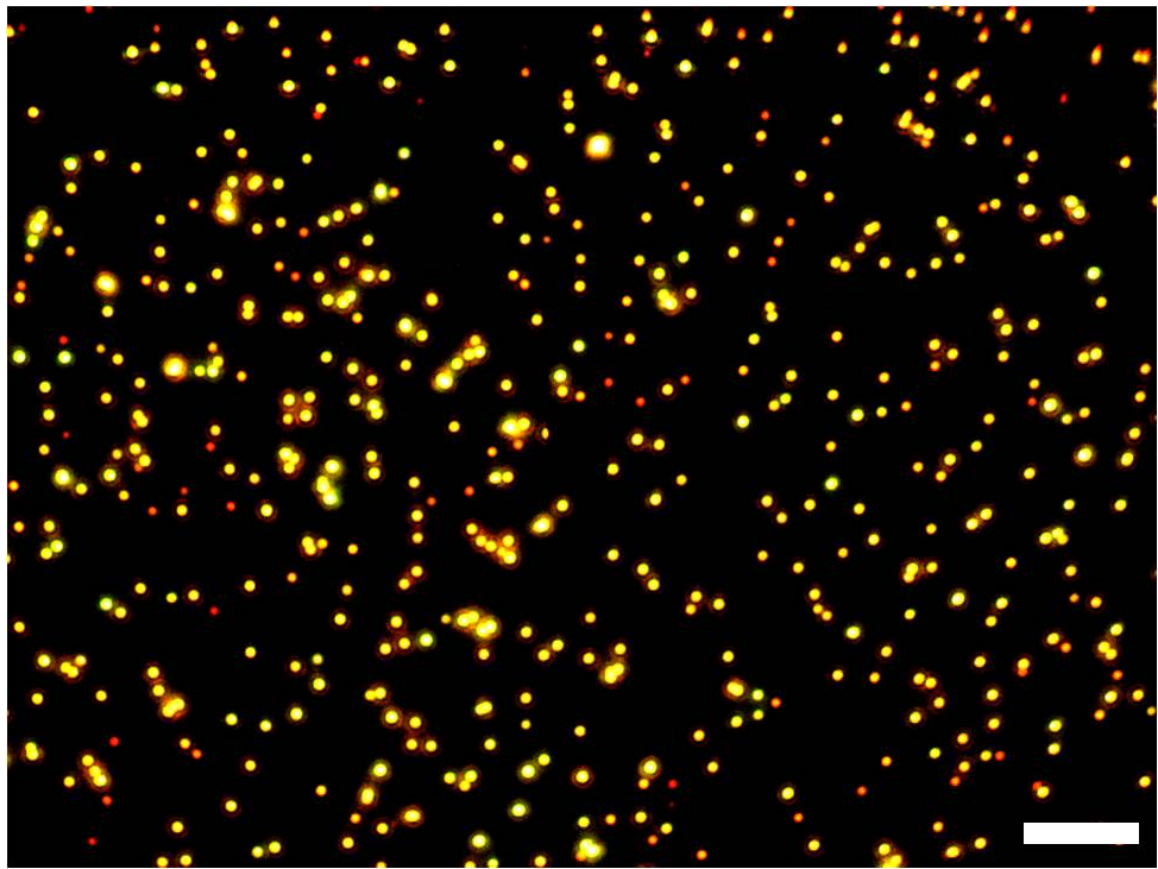


**Figure S12.** Far-field dark-field scattering image of gold NRs deposited on a glass cover slip. The dimensions of the NRs are  $(140.0 \pm 5.0)$  nm x  $(84.7 \pm 3.7)$  nm (the same sample shown in Figures 6g-i and Figure S9). Scale bar: 10  $\mu$ m.

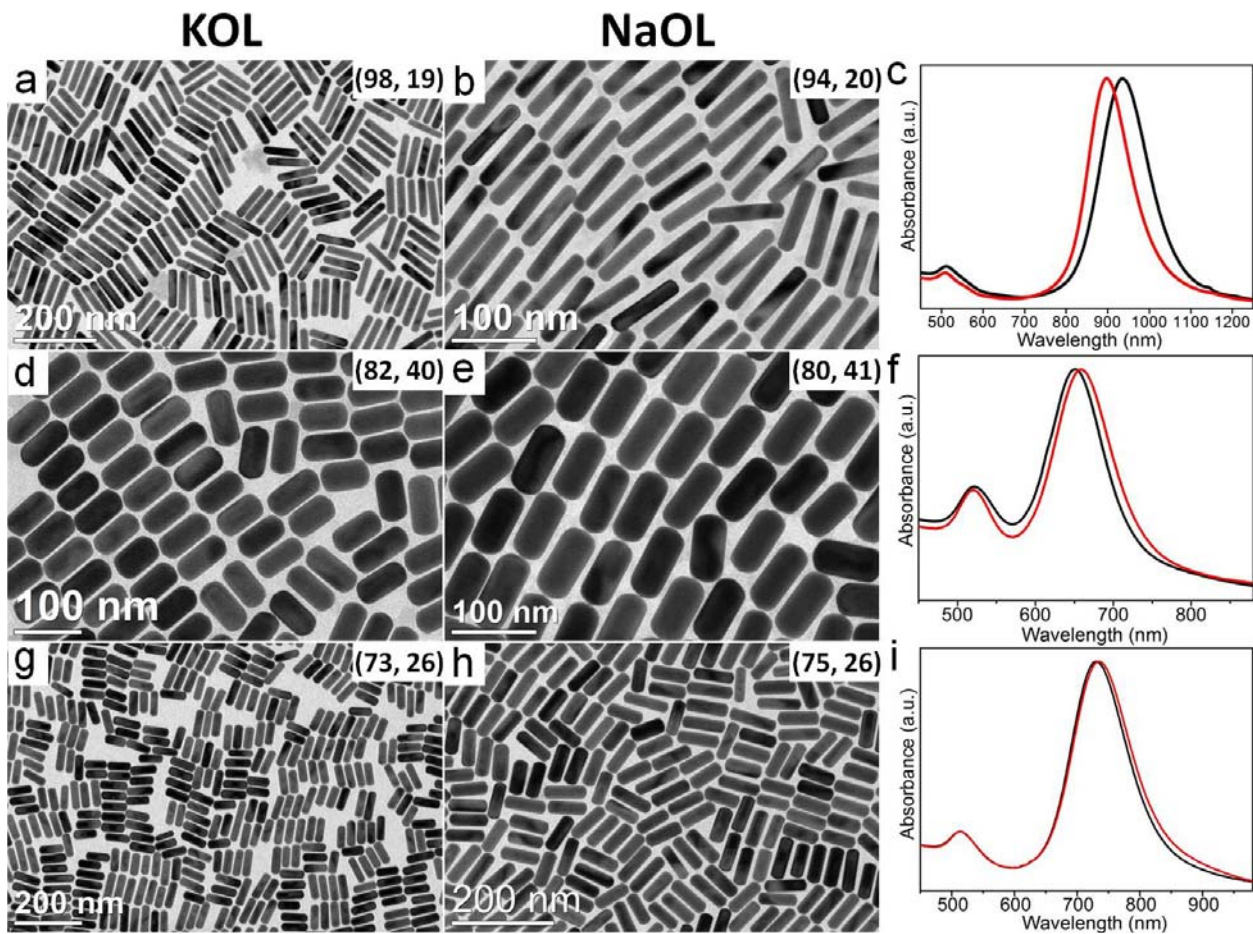


**Figure S13.** (a, b) TEM images of gold NRs synthesized using identical growth conditions as detailed in Table S2 except with (a) 1.303 g of potassium oleate (KOL) and (b) 1.234 g of NaOL. (c) Normalized extinction spectra of gold NRs shown in a (black curve) and b (red curve). (d, e) TEM images of gold NRs synthesized with (d) 1.629g of KOL and (e) 1.543g of NaOL. Other synthetic parameters are: 9.0 g of CTAB, 12 mL of 4 mM AgNO<sub>3</sub> solution, 0.4 mL of seed solution and 1.5 mL of HCl. (f) Normalized extinction spectra of gold NRs shown in d (black curve) and e (red curve). (g, h) TEM images of gold NRs synthesized with (g) 1.629 g of KOL and (h) 1.543 g of NaOL. Other synthetic parameters are: 9.0 g of CTAB, 12 mL of 4 mM AgNO<sub>3</sub> solution, 0.4 mL of seed solution and 2.1 mL of HCl. (i) Normalized extinction spectra of gold NRs shown in d (black curve) and e (red curve). Insets are the average length and diameter (in nm) of the NRs determined by measuring the dimensions of at least 50 NRs from their TEM images.

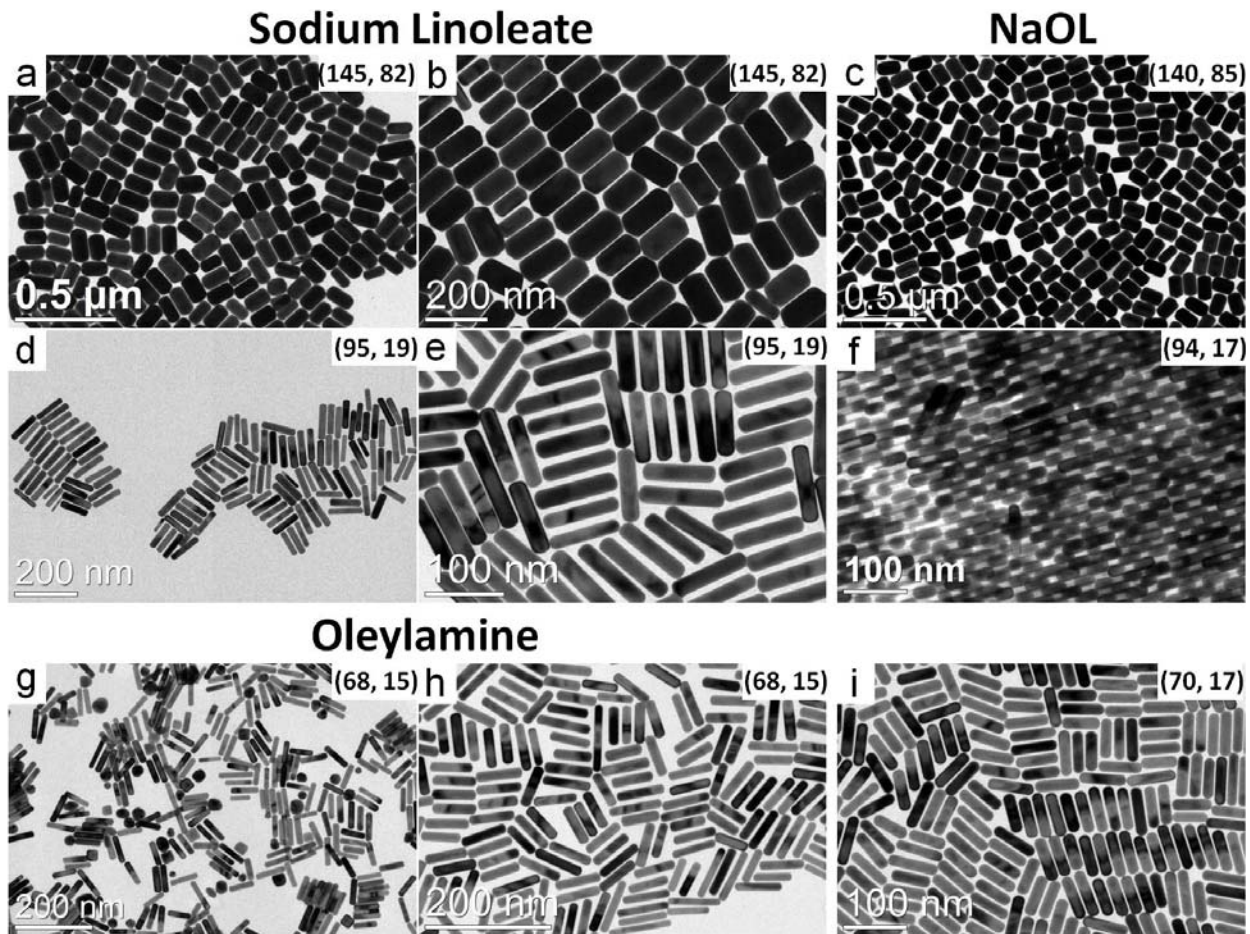


**Figure S14.** (a-c) TEM images of gold NRs synthesized using identical growth conditions as detailed in Table S5 except with (a, b) 1.234 g of sodium linoleate and (c) 1.234 g of NaOL. (d-f) TEM images of gold NRs synthesized using identical growth conditions as detailed in Table S2 except with (d, e) 1.234 g of sodium linoleate and (f) 1.234 g of NaOL. (g-i) TEM images of gold NRs synthesized using identical growth conditions as detailed in Table S2 except with (g, h) 4 mmol of oleylamine and (i) 1.234 g of NaOL.

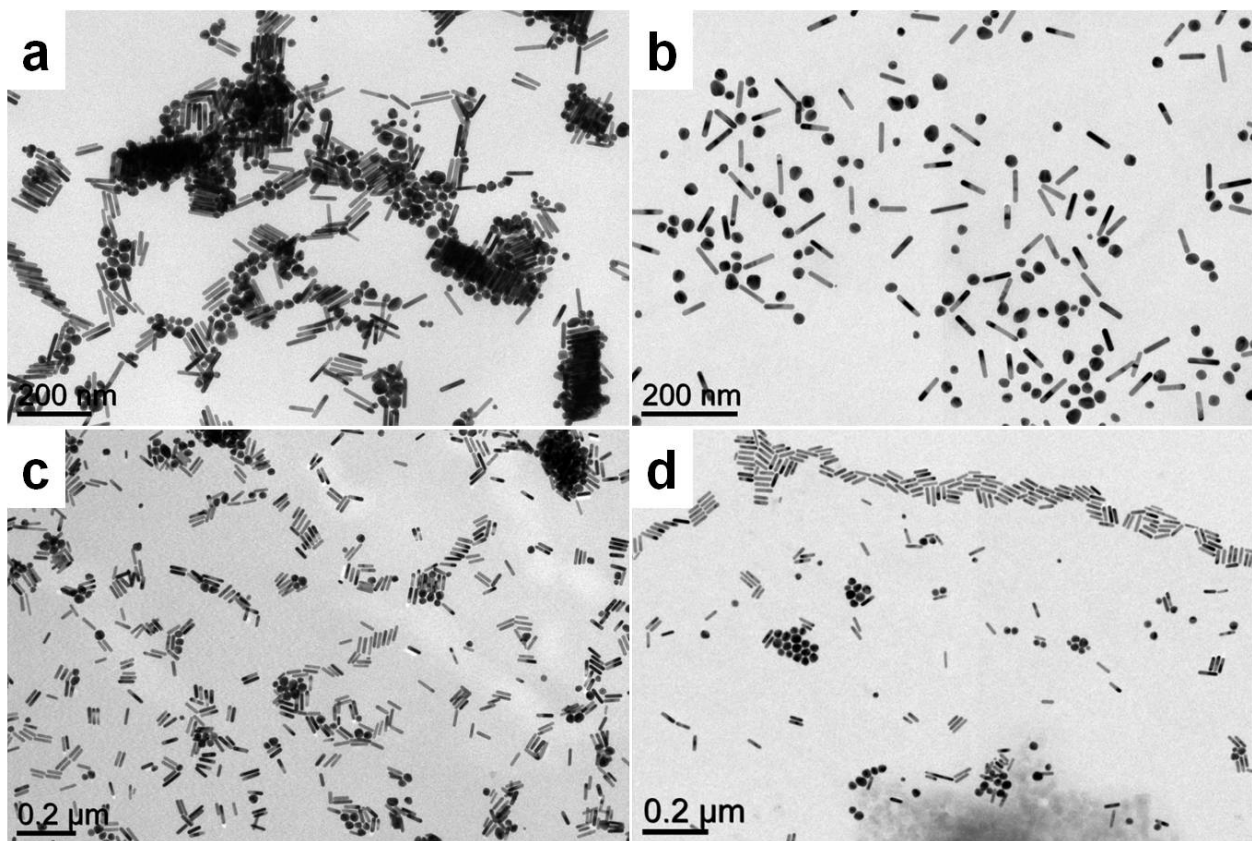


**Figure S15.** TEM images of gold NRs synthesized by replacing NaOL with same amount of sodium stearate. 4.5 mL of 0.064 M AA was used for all reactions to ensure complete reduction of  $\text{Au}^{3+}$  before injection of seed particles. Other synthetic parameters are: (a) 7.0 g of CTAB, 12 mL of 4 mM  $\text{AgNO}_3$  solution, 0.8 mL of seed solution, 2.1 mL of HCl and 1.553 g of sodium stearate. (b) 9.0 g of CTAB, 18 mL of 4 mM  $\text{AgNO}_3$  solution, 0.4 mL of seed solution, 1.5 mL of HCl and 1.242 g of sodium stearate. (c) 9.0 g of CTAB, 12 mL of 4 mM  $\text{AgNO}_3$  solution, 0.2 mL of seed solution, 1.5 mL of HCl and 1.553g of sodium stearate. (d) 9.0 g of CTAB, 12 mL of 4 mM  $\text{AgNO}_3$  solution, 0.4 mL of seed solution, 1.5 mL of HCl and 1.553g of sodium stearate.

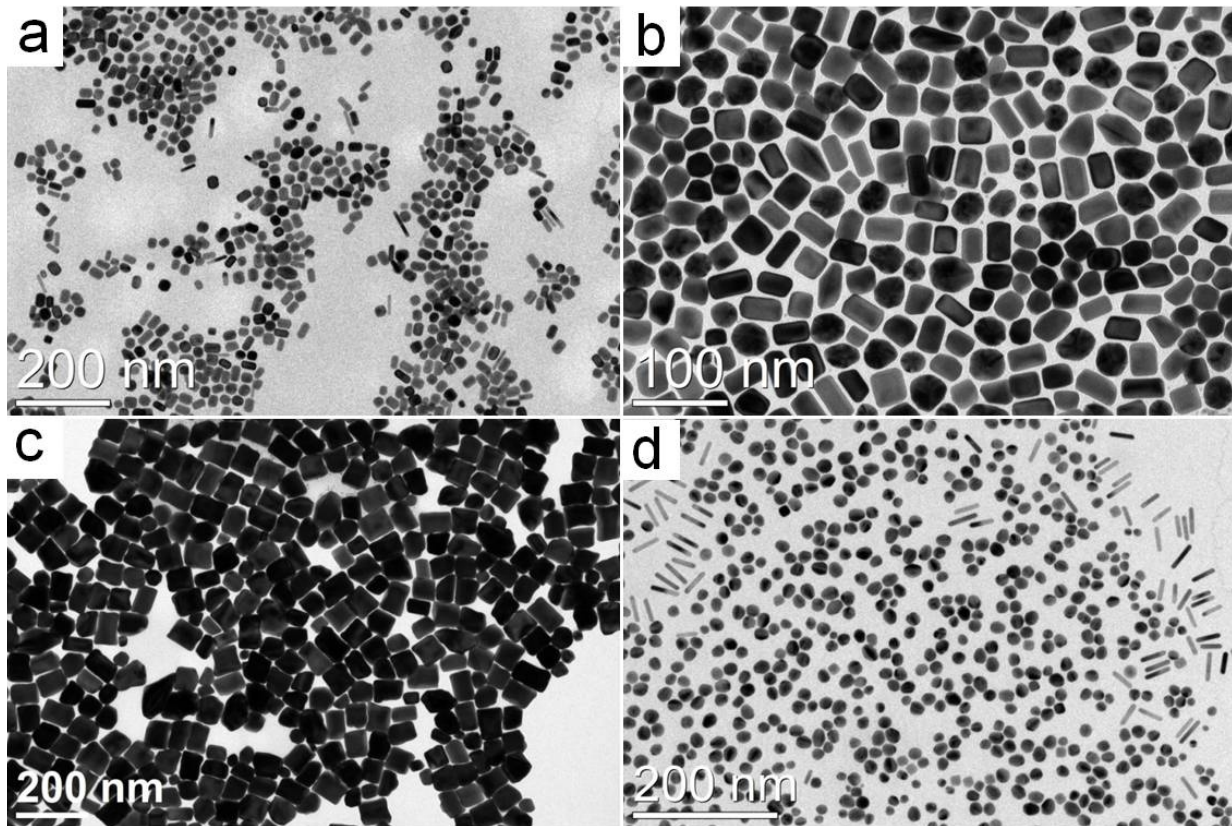


**Figure S16.** (a-c) TEM images of gold nanocrystals synthesized using 9.0 g of CTAB, 1.543 g of NaOL and 1.25 mL of 0.064 M AA in the growth solution but without the addition of HCl. pH of these growth solutions are measured to be around 5.8 (Table S1). Other synthetic paramters are: (a) 12 mL of 4 mM AgNO<sub>3</sub> solution, 0.8 mL of seed solution. (b) 24 mL of 4 mM AgNO<sub>3</sub> solution, 0.2 mL of seed solution. (c) 12 mL of 4 mM AgNO<sub>3</sub> solution, 0.01 mL of seed solution. (d) TEM image of gold NRs synthesized with 9g of CTAB (0.047 M), 24 mL of 4 mM AgNO<sub>3</sub> solution, 0.4 mL of seed solution, 2.1 mL of HCl and 4.5 mL of 0.064 M AA in the growth solution. pH of the growth solution was measured to be 1.30. It is apparent that with comparable acidity of growth solution, reducing the amount of seed particles under 0.047M CTAB does not lead to the same level of control as CTAB (0.047M)—NaOL system. Gold NRs synthesized using the same growth conditions as (d) except with additional 1.234 g of NaOL can be found in Figure S4.

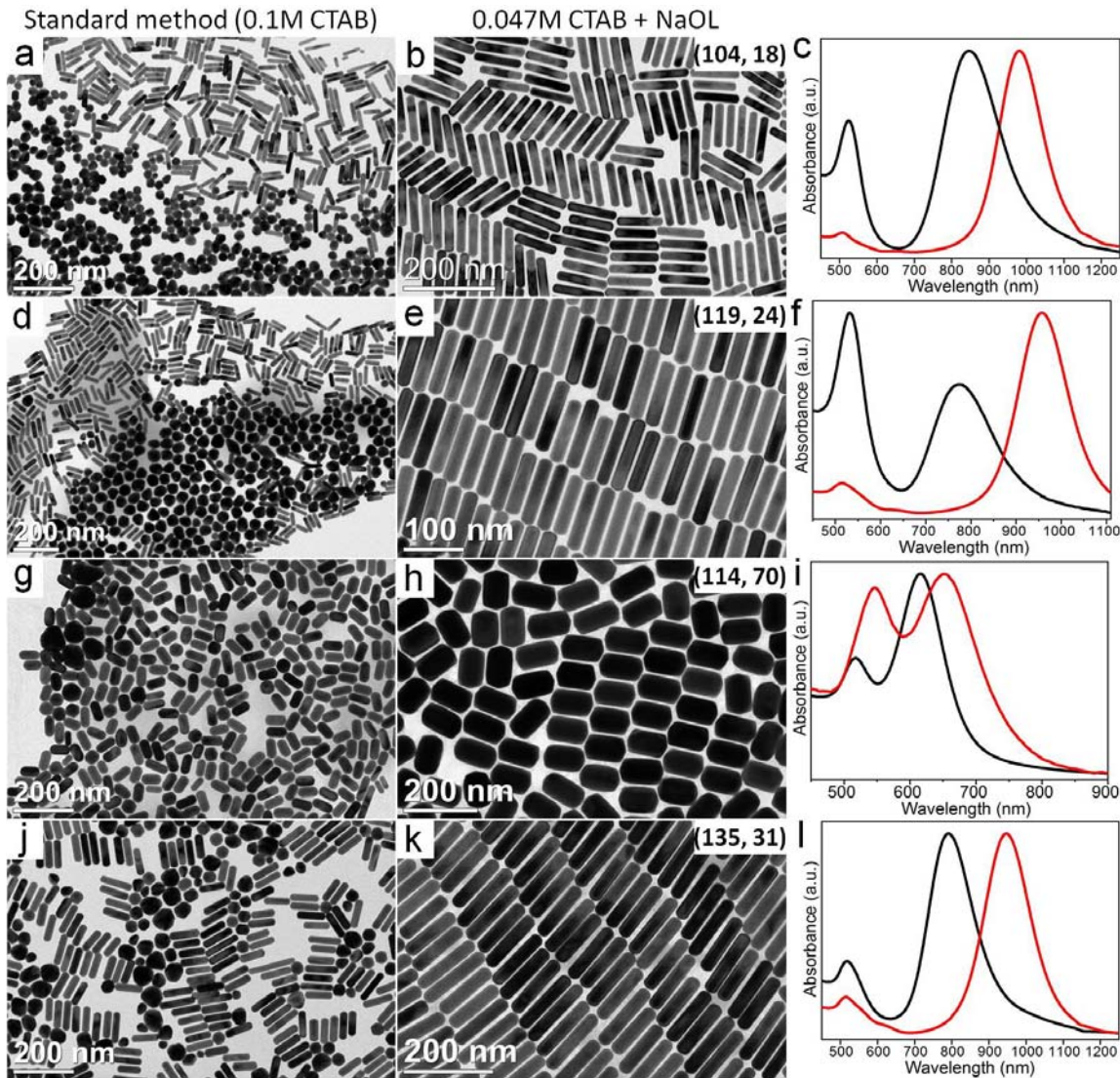


**Figure S17.** Comparative studies of size uniformity and dimensional tunability of gold NRs synthesized using 0.1 M CTAB (left column) vs. 0.047 M CTAB-NaOL system (middle column). 4.5 mL of 0.064 M AA were used for samples shown in the left column while 1.25 mL of 0.064 M AA were used for samples shown in the middle column. Other synthetic parameters are: (a, b) 24 mL of 4 mM AgNO<sub>3</sub> solution, 0.4 mL of seed solution, 2.3 (a) and 2.1 (b) mL of HCl. (d, e) 24 mL of 4 mM AgNO<sub>3</sub> solution, 0.2 mL of seed solution, 2.3 (d) and 2.1(e) mL of HCl. (g, h) 12 mL of 4 mM AgNO<sub>3</sub> solution, 0.05 mL of seed solution, 1.7 (g) and 1.5 (h) mL of HCl. (j, k) 24 mL of 4 mM AgNO<sub>3</sub> solution, 0.05 mL of seed solution, 3.3 (j) and 3.0 (k) mL of HCl. 1.234 g of NaOL were used for (b, e, k) and 1.543g of NaOL for (h). (c, f, i, l) Normalized extinction spectra of gold NRs shown in the corresponding rows synthesized using 0.1 M CTAB (black curves) and 0.047 M CTAB-NaOL system (red curves).

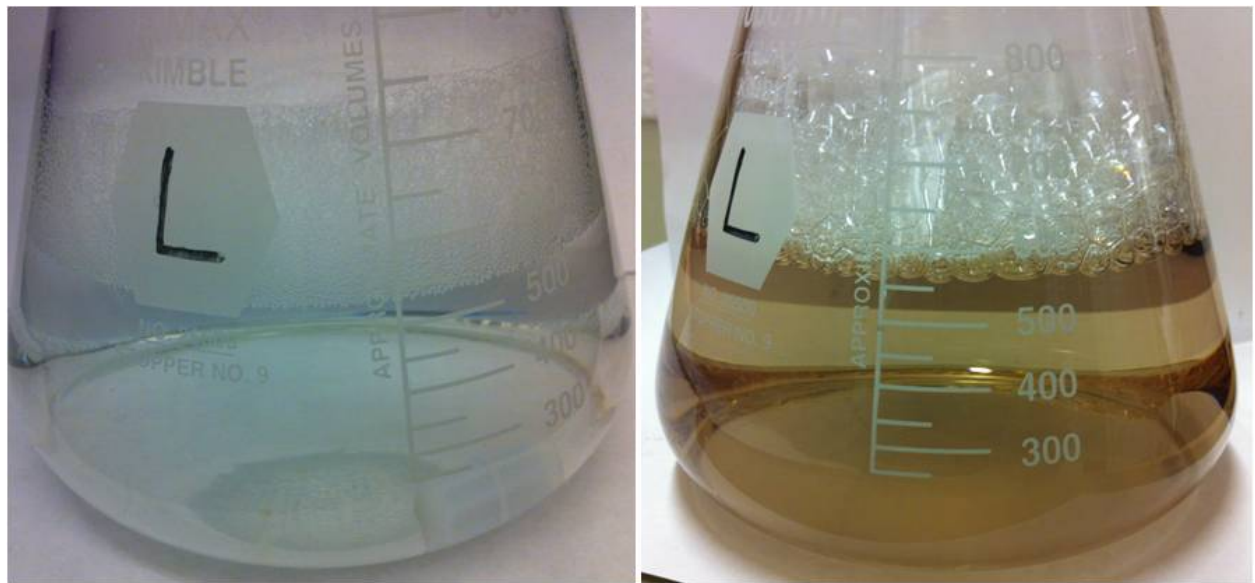


**Figure S18.** (Left) Photograph of the colorless reaction mixture 90 min after the addition of  $\text{HAuCl}_4$ . NaOL molecules reduces  $\text{Au}^{3+}$  to  $\text{Au}^+$  and AA has not been added to the growth solution at this point. (Right) Photograph of the reaction mixture 120 min after the injection of seed particles. 2.1 mL of HCl was employed for this reaction. The absence of a reddish hue in the growth solution is indicative of a very low concentration of spherical shape impurities.

**Table S6.** Comparison of dimensions of gold NRs synthesized under identical growth conditions except with different amounts of NaOL.

CTAB (g)	AgNO <sub>3</sub> (mL)	Seed (mL)	HCl (mL)	NaOL (g)	Average length (nm)	Average diameter (nm)	Figure number
9.0	18.0	0.2	3.0	1.543	109.5±5.7	27.3±1.9	S2e
9.0	18.0	0.2	3.0	1.234	118.4±8.3	22.7±1.6	S6
9.0	24.0	0.4	2.1	1.543	92.2±4.8	22.1±1.1	S2f
9.0	24.0	0.4	2.1	1.234	104.3±5.0	18.0±0.6	S4
9.0	18.0	0.2	2.1	1.543	99.1±6.1	35.7±2.0	S7b
9.0	18.0	0.2	2.1	1.234	98.2±6.2	23.8±1.1	S6
9.0	24.0	0.2	1.5	1.543	113.7±6.2	41.8±2.4	3b, S7g
9.0	24.0	0.2	1.5	1.234	111.8±5.0	33.2±1.3	3h, S7c
9.0	24.0	0.2	2.1	1.543	105.0±5.7	32.2±1.7	3g
9.0	24.0	0.2	2.1	1.234	119.0±7.0	24.0±1.4	S4, S6
9.0	24.0	0.2	3.0	1.543	113.8±5.4	25.2±1.2	S7h
9.0	24.0	0.2	3.0	1.234	126.2±6.9	23.7±1.1	S4, S6
7.0	12.0	0.8	2.1	1.543	109.2±9.1	54.4±3.0	S8a
7.0	12.0	0.8	2.1	1.234	91.7±4.3	41.8±2.2	3a
9.0	24.0	0.1	1.5	1.543	115.7±5.9	47.9±1.9	5e
9.0	24.0	0.1	1.5	1.234	125.0±5.5	40.1±1.9	3f
9.0	24.0	0.01	3.0	1.543	163.0±10.7	74.9±4.0	5f
9.0	24.0	0.01	3.0	1.234	171.9±12.3	48.9±3.0	S8c, S8d
9.0	18.0	0.4	1.5	1.543	88.2±4.0	40.0±1.6	S10i, S10j
9.0	18.0	0.4	1.5	1.234	86.7±5.1	20.0±1.4	S5
9.0	18.0	0.2	1.5	1.543	105.3±4.5	49.9±2.0	6a, S11h, S11i
9.0	18.0	0.2	1.5	1.234	94.1±4.3	24.2±1.0	S5